MODELING PTFE WELDING TO REDUCE CYCLE TIMES: FINITE DIFFERENCE METHOD FOR 2-D TRANSIENT HEAT CONDUCTION

by

Joel Thompson

A Thesis

Submitted to the Faculty of Purdue University

In Partial Fulfillment of the Requirements for the degree of

Master of Science in Engineering

School of Mechanical Engineering

Fort Wayne, Indiana

August 2019

THE PURDUE UNIVERSITY GRADUATE SCHOOL
STATEMENT OF COMMITTEE APPROVAL

Dr. Zhuming Bi, Chair

Department of Civil and Mechanical Engineering

Dr. Nashwan Younis

Department of Civil and Mechanical Engineering

Dr. Donald Mueller

Department Civil and Mechanical Engineering

Approved by:

Dr. Hosni Abu-Mulaweh

Head of the Graduate Program

This thesis is dedicated to Charlotte, my loving and patient wife who supported me throughout this process.

ACKNOWLEDGMENTS

I would like to thank Dr. Bi and Dr. Mueller of Purdue University Fort Wayne's Mechanical Engineering faculty for their guidance throughout this project. They gave me the guidance necessary to successfully complete my work. I would also like to thank Dr. Younis for his support throughout my collegiate career and always having an open door to his office to talk about Nebraska football.

Next, I would like to thank the operators Rob, Will, and Kevin for their help and expertise in the PTFE welding manufacturing process. Their help was greatly appreciated for answering any questions about the process as well as running validation tests with the thermal camera.

I would like to thank Chris Gardner for helping me understand the current manufacturing process through his knowledge and experience in the subject.

Eric Simmerman was a great help in demonstrating how to use the FLIR thermal camera and its corresponding software. Without his time and help, the process would have been much harder.

I would like to thank Tim McCulfor, Dan Martin, Tony Perugini, and any other supporting personnel in the material test lab. Their help with answering my questions about material properties of PTFE was greatly appreciated and necessary for this project.

Last but certainly not least, I would like to thank my wife and my family for their support throughout not just my master's degree but all of my collegiate career. Their encouragement has and always will mean the world to me.

Praise God, my Lord and my Savior for giving me the strength and the perseverance for this project. May all of the glory go to him.

TABLE OF CONTENTS

LIST OF TABLES

LIST OF FIGURES

LIST OF SYMBOLS AND ABBREVIATIONS

L	Length, m
H	Height, m
M	Nodes in X direction
N	Nodes in Y direction
dx	Distance between nodes in X direction, m
dy	Distance between nodes in Y direction, m
dt	Change in time for transient time step, s
T_1	Initial temperature, °C
T	Temperature, °C
T'	Temperature of next time step, °C
A	Area of Heater die assembly, m^2
q	Heat flux, W/m^2
q_1	Heat flux on top and bottom boundaries, W/m^2
q_2	Heat flux on side boundary, W/m^2
q_s	Surface heat flux for semi-infinite analysis, W/m^2
q_p	Heat Flux over time, W/m^2
c_1	Constant of initial heat flux calculation
c_2	Constant of transient heat flux calculation
Q	Heat Loss, Power, W
R	Ramp time for heat flux, min
RT	Ramp time in units of dt, 0.1s
F_o	Fourier Number
k	Thermal Conductivity, W/m-K
C_p	Specific Heat, J/kg-K
ρ	Density, kg/m^3
α	Thermal Diffusivity, m^2/s
α	Thermal Expansion, m/m/°F
V	Volume, m^3
V_o	Initial Volume, m^3
$PTFE$	Polytetrafluoroethylene
MTL	Material Test Lab

ABSTRACT

Author: Thompson, Joel, T. MSE
Institution: Purdue University
Degree Received: August 2019
Title: Modeling PTFE Welding to Reduce Cycle Times: Finite Difference Method for 2-D Transient Heat Conduction
Committee Chair: Zhuming Bi

This project investigated the manufacturing of large diameter welded PTFE rings. This welding process is time consuming and can take over ten hours for one complete weld cycle. Additionally, the welds can have poor quality in the center of the material due to insufficient heating across the weld face. The goal of this research was to address these two issues by analyzing the current process to determine the root cause of weld failures while also determining the feasibility of reducing the weld cycle time. The scope of this thesis was to develop a model to better understand and simulate the current process which could then be used for design future improvements.

A MATLAB model of the current process was developed to simulate the transient heating cycle of the most common weld cycle for PTFE currently used by a manufacturer of PTFE seals. The data for the material properties was gathered from the manufacturer test data as well as from Lau et al. (1984). Temperature dependent material properties were used in the program because the PTFE is heated above its melting point during the weld cycle. Because of the complexity of this heat transfer problem, the heat flux in the model was tuned so that it accurately reflected the current process. This is because the goal of this study was not to determine the exact heat flux as it was unknown, but to develop an accurate model. Thus, the heat flux was assumed and the model was then verified with process data. Results from the model were compared to validation results from a FLIR thermal camera. The model predicted the compared temperatures to within 3.1% error at both 15-minute and 90-minute intervals. Though there are many potential sources of error in the process and the thermal camera measurement, the model was deemed acceptable as a model of the current process. A semi-infinite heat analysis was calculated to simulate a hot plate welding method on the PTFE. This showed that the temperature of the weld face could be raised by 57.275°C. It is believed that a method similar to hot plate welding applied to PTFE could heat the material faster and more evenly than the current process, reducing the weld failures and cycle time.

1. INTRODUCTION

This project was performed in conjuncture a leading manufacturer of thermoplastic sealing products. For proprietary purposes, the company name will not be mentioned. This company is an international supplier of highly engineered precision plastic seals. With 9 research & development centers, 28 manufacturing facilities, and 53 marketing sites internationally, the company is a leader in the world of thermoplastics. The Fort Wayne location focuses on industrial and aerospace products for high performance sealing applications. The focus of manufactured products include elastomer energized thermoplastic seals with the focus being on Polytetrafluoroethylene, or PTFE products.

PTFE seals are produced in a large array of sizes ranging from less than a quarter of an inch to over twelve feet in diameter. At this manufacturer, all the proprietary powder is blended and molded in house for the seals to be manufactured. The powder is either compression or shell molded; however, due to the cost of large tooling, extremely large rings of material cannot be molded. When the seal diameter to be manufactured is greater than about 40 inches in diameter, a welding process is involved to create the large rings. In this welding process, a ring of 40 inches is molded and then cut. This ring is then joined through the welding process to other cut rings to create a ring of the desired diameter. The welding cycle that is used is based on the material of the ring to be welded. For the most commonly welded materials, the welding cycle that is used takes a total time of over 10 hours to complete with about 5 hours of total heating time. This means that one weld generally takes over an entire shift to complete. Moreover, a single welded ring can take up to about 4 or 5 total welds to complete depending on the desired finished diameter of the welded ring. For example, a welded ring requiring 4 total welds would take over 40 hours of total cycle time. This means that one welded ring could potentially take over 2 to 6 days to complete depending on how many shifts are operating the welders at a given time. These rings are then machined on a large CNC lathe in which they may produce about 10 to 15 parts per ring dependent on the thickness of the part being machined. Therefore, for orders of many parts, numerous rings would need to be manufactured. The amount of time that is consumed in cycle times to produce large diameter parts is extremely high given this current operations method. This study aimed to analyze the current method of production to determine if there is a more cost-effective solution. The goal of this project was to gain a better understanding of the current process and to determine

the feasibility of reducing the weld cycle times. To gain a better understanding of the current process, the current welding operation was modeled as a 2-D transient heat conduction problem using the finite difference method. The means by which this problem was modeled was using the program MATLAB. The majority of this paper explains the building process and validation of the 2-D transient heat conduction MATLAB model. Using this model, potential design changes such as increased power and a hot plate welding method were analyzed to see if the cycle time of the welding process could be reduced. One of the methods that was not considered for reducing the cycle time was changing the cooling time. This was not considered as changing the cooling time can change the material properties of the PTFE being welded. Although the goal of the problem was to reduce the overall cycle time, it was pertinent for the material properties of the PTFE to remain unchanged. Therefore, changing the cooling times was not considered, and the focus of the project was on the heating phases of the material.

The material properties of PTFE were greatly investigated for this project to see how they would be affected by parameters in the welding process. Properties of thermoplastics and thermosets were compared as PTFE has properties of both. Also explored were other welding techniques of common thermoplastics. The Literature Review discusses current joining processes of thermoplastics. Also explained are the differences between PTFE and most other thermoplastic materials.

2. LITERATURE REVIEW

2.1 Intro to Thermoplastics

In today's industry, thermoplastics are gaining an increasing role in a wide variety of applications including automotive, aerospace, industrial, and many more. They are becoming more and more popular because of their favorable characteristics. To name a few, thermoplastics generally have a high density, high modulus of elasticity, corrosion resistance, electrical properties, as well as lower manufacturing costs than metals (Troughton, 2008). Thermoplastics melt when heated and thus are preferred for most manufacturing methods. Some plastics are melt-processible and can be melted and re-melted, whereas other plastics cannot be melted but just degrade when heated. These types of plastics are separated into two groups that will be discussed in detail: Thermosets and Thermoplastics. Such a wide variety of materials make it possible to select the best material for a specific application and even to customize materials for a certain application.

2.1.1 Thermoplastics vs Thermosets

Most everyone is familiar with plastics; however, under the term plastics, there are two classes of plastics that are very different from each other. The major types of plastics are thermosets and thermoplastics. The biggest distinction between the two groups is the fact that thermosets cannot be melted. When thermosets are heated to a high enough temperature, they do not melt but degrade (Ritter et al. 2015). This degradation is due to the irreversible process that thermosets undergo called vulcanization which will be further discussed.

Thermoplastic materials on the other hand can be melted and formed. Both types of plastics are polymeric materials, but there are differences between their polymer chains that distinguish the two from each other. Polymers in general have large molecular structures with repeating units or blocks of the polymer chain. The repeating units make up the molecular structure of the polymer. Polymers are also made of organic chemicals such as polyolefins, fluorocarbons, or styrene for example. These two distinctions are what classifies a material as a polymer: they are made of organic materials and have large, repeating molecular structures (Ebnesajjad, 2015). The networks of the polymer chain can be either three dimensional or one dimensional. Thermosets have chains that are made up of three-dimensional chain matrices (American Chemistry Council, 2018). Unlike thermoplastics, thermosets must be cured, or vulcanized when they are manufactured.

They must undergo an irreversible chemical process in order to form the bond to give the material its characteristics. The vulcanization process requires the material to be cured by heat, catalysts, or ultraviolet light. During this vulcanization process, the monomer chains are crosslinked to form the polymer chains. The curing process allows the cross linking between polymer chains to take place (Dodiuk, 2014). Thermoplastics do not require this curing or vulcanization process and can be melted, formed, and re-melted. Although the curing process is not required for thermoplastic materials, they still must undergo a process that gives the material its properties. For many plastics, this is called crystallization. Thermoplastic materials can be further classified as either amorphous or semi-crystalline materials. PTFE is a semi-crystalline material that becomes crystalline through a sintering process. Exact sintering process times and temperatures depend on the specific material, but generally have lengthy heating and cooling times up to 20 hours. The crystalline structure of PTFE helps to give it its strength as will be further discussed in the Fluoropolymers section.

2.1.2 Fluoropolymers

Fluoropolymers are polymer materials that consist of fluorine (F) and carbon (C) (Ebnesajjad, 2015). Within this category there are also distinctions of fully fluorinated polymers and partially fluorinated polymers. Fully fluorinated polymers are also called per-fluoropolymers. PTFE is a linear fluoropolymer. As discussed earlier with the polymer molecule chains, PTFE has a linear, one dimensional molecular structure. The molecular structure of PTFE is built on a chain of carbon atoms with fluorine atoms attached to the carbon atoms. Figure 1 below shows the representation of the molecular chain.

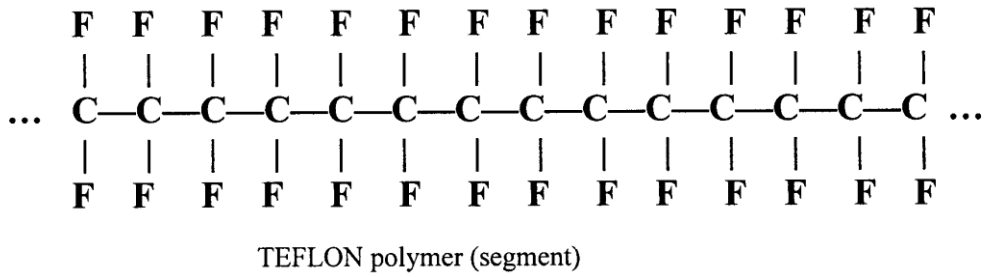

TEFLON polymer (segment)

Figure 1: Linear molecular structure of PTFE built with a chain of Carbon atoms protected by Fluorine atoms ("Wordpress", 2016)
https://teflon2016.wordpress.com/2016/09/04/chemicool-polytetraflouroethene/

Because the chain is built from carbon and fluorine atoms, polymers tend to have properties that are common to these two elements. Fluoropolymers are built from bonds between carbon and fluorine atoms as well as additional covalent bonds if any. In materials with more covalent bonds, the material tends to become weaker as the material becomes more perfluorinated (Ebnesajjad, 2015). However, PTFE has a linear chain of atoms. With this linear structure, PTFE tends to have extremely desirable strength properties. The structure of the molecules of PTFE is built on carbon – carbon bonds and carbon – fluorine bonds. These bonds are extremely strong and have bond energies C-C = 607 kJ/mol and C-F = 552 kJ/mol (Ebnesajjad, 2015). This molecular structure gives PTFE some of its favorable characteristics. With the carbon rod surrounded by the fluorine atoms, the carbon-carbon bonds are protected by the surrounding fluorine atoms. This structure provides chemical resistance as well as stability in the molecule. The fluorine atom shield around the carbon atoms also provides PTFE with a low surface energy as well as a very low coefficient of friction, 18 dynes/cm dynamic and 0.05-0.08 static respectively (Ebnesajjad, 2015). Due to the uniform fluorine shield around the carbon atoms, PTFE is not polarized as a material and has favorable electrical properties. Due to these contributing factors, PTFE is a very versatile and ultimate fluoroplastic material.

2.1.3 Favorable Properties of Thermoplastics

Thermoplastics are preferred materials for applications when metal is too abrasive or heavy. Thermoplastics provide high strength as well as ductility in their applications. Because of their molecular weight, thermoplastics are much lighter in general than metals, but still provide the necessary strength in most applications. They are also generally easily manufacturable. PTFE however has the highest molecular weight of all thermoplastics, and thus lends itself difficult to most thermoplastic processing methods.

2.1.4 Common Uses of Thermoplastics

Thermoplastics are used in such a wide variety of applications that they are too numerous to mention. Plastics are generally preferred when metal is either too heavy or too abrasive, and when high thermal and elastic properties are needed in the application. Thermoplastic seals are used in abundant applications including aerospace, automotive, and industrial to name the biggest three. Commonly manufactured thermoplastic sealing materials include PTFE, polyurethanes,

nylon, PEEK, and UHMW-PE. However, the material that is by far used the most is PTFE. Variations of PTFE compounds exist by customizing the amounts of additives and fillers in order to obtain a certain set of characteristics. The combinations of these additives and fillers will not be shared as that is confidential information; however, some of the common filler types are carbon fibers, glass, and bronze. The types of filler materials used affect the properties of the material. This also affects the welding cycle that would be used.

2.1.5 Properties of PTFE

As mentioned previously, PTFE is a very durable material which makes it useful for a variety of applications. In particular, PTFE has a very high tensile strength of 29-39 MPa. This is due to the large molecular chains previously mentioned that give the material its strength. PTFE also has the lowest coefficient of friction of almost any material. Therefore, it is desirable for sealing applications and guide bearings to reduce the friction and heat buildup in a sealing system. In addition to its favorable mechanical properties, PTFE has extremely durable chemical and thermal properties as well. It is corrosion resistant to many materials. It also has a very high melting point which allows it to be placed in high heat applications where other thermoplastics could not be used. Also important for withstanding high heat applications is the fact that PTFE has very poor thermal conductivity. This in particular makes the material one of the hardest to process. PTFE does not melt and flow like other thermoplastics due to its molecular weight, but rather it reaches a gel state when it is heated above its melting point. If held at a high temperature above its melting point, generally above 340°C, the material begins to degrade. With thermoplastics, the higher the molecular weight of the material, the harder it is to be melt processible. Though PTFE is a thermoplastic, it is manufactured differently compared to common thermoplastics.

2.2 Manufacturing Methods

Typical manufacturing processes of plastics were investigated to validate that the most effective and efficient process was being used. There are three main categories of joining plastics: mechanical assembly, bonding, or welding. These categories can further be broken down into specific methods as shown in Figure 2. These joining methods will be further discussed in the following sections.

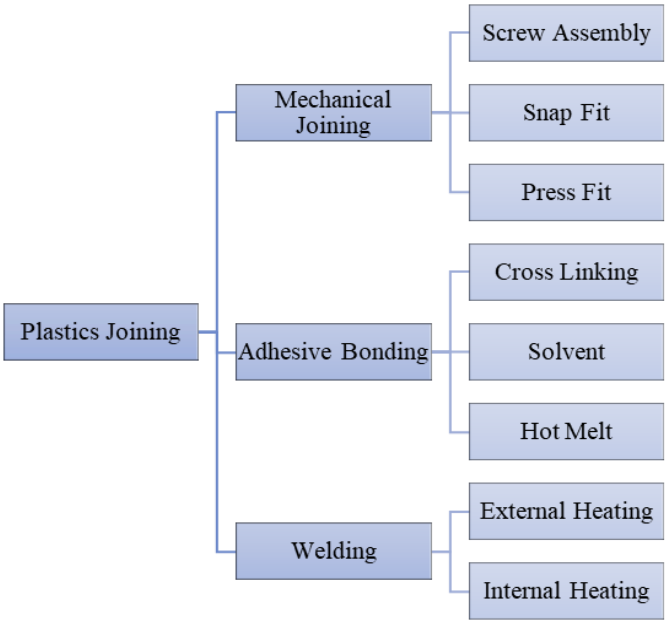

Figure 2: Overview of plastics joining methods

All methods of plastics joining were briefly studied to determine if there is a better suited method for joining PTFE for the specific application. The next sections discuss these methods.

2.2.1 Joining Methods

2.2.1.1 Mechanical Assembly

As shown in the figure, there are various methods of mechanical joining and adhesive bonding with screw assembly, snap fit, and press fit to name a few. For the application discussed in this paper, the goal is to join large pieces of PTFE which will then be machined on a CNC lathe. This requires that the joining must be permanent enough to withstand machining. Also, the application of the end product is to be installed in a high precision sealing application. Thus, it is very critical that the method of joining produces a seamless and mechanically sound joint equal to the strength of the material being joined. As discussed in Fluoroplastics on page 456, the method of mechanical assembly is applicable for low loads, but does not produce a joint that is equal to the strength of the material (Ebnesajjad, 2015). Thus, for sealing applications, a stronger joint than a mechanically assembled joint is necessary.

2.2.1.2 Bonding

Another method of joining plastics is adhesive bonding. In this method, the surfaces of the materials are chemically joined to one another through the use of solvents or etching processes. PTFE is adherently difficult to bond due to its very low coefficient of friction. Although an etching process is currently used to bond another product type, this process is not applicable in this situation as it would not be a strong enough joint for machining. Etching is generally used to join PTFE to another material surface through the use of a special glue or bonding agent. However, this is not applicable to bond PTFE to itself for the case in discussion. Using this type of bonding method would not create a strong enough joint for a machining process. Thus, in order to produce a strong, homogenous joint in the PTFE bar to be machined, it must be joined by a welding process.

2.2.2 Welding

As shown in Figure 2, welding methods can be categorized as either external heating or internal heating. Welding methods can further be broken down into more specific methods as shown below in Figure 3.

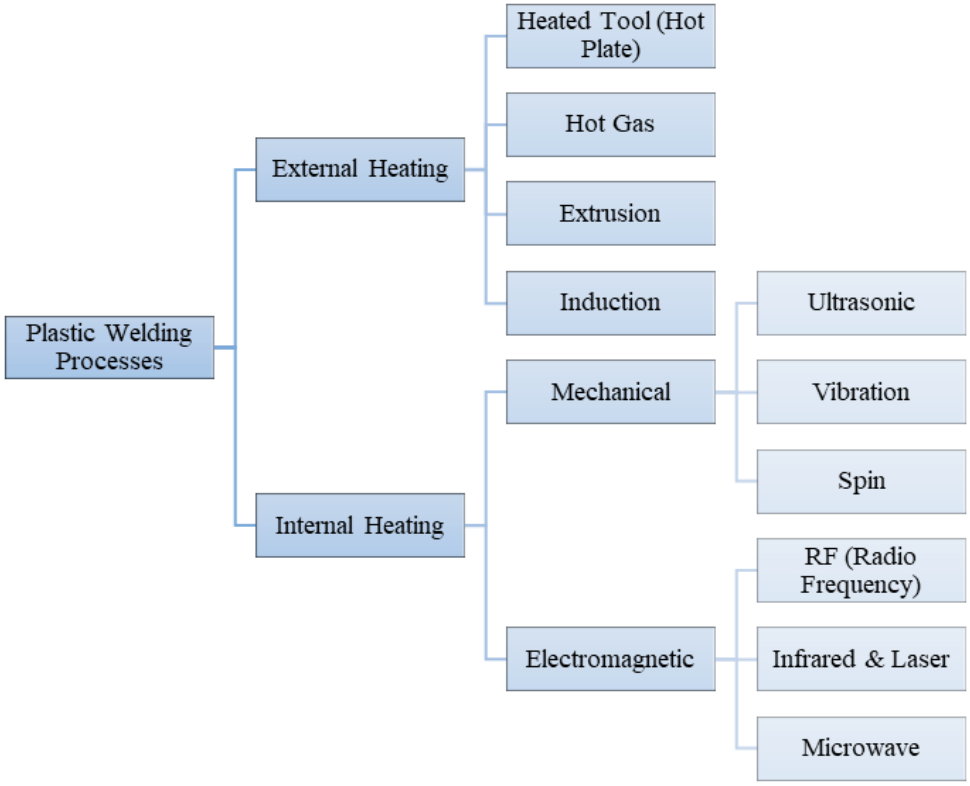

Figure 3: Thermoplastic welding methods

Figure 3 shows an overview of the commonly used welding methods of thermoplastics used in industry. Welding methods can be categorized as either internal or external heating. From there, internal heating can be broken down even further into electromechanical or mechanical heating methods. Although there are a large variety of welding methods for thermoplastics, they all have similar phases when it comes to the necessary steps to make a weld. The phases of welding and their description are represented in Figure 4.

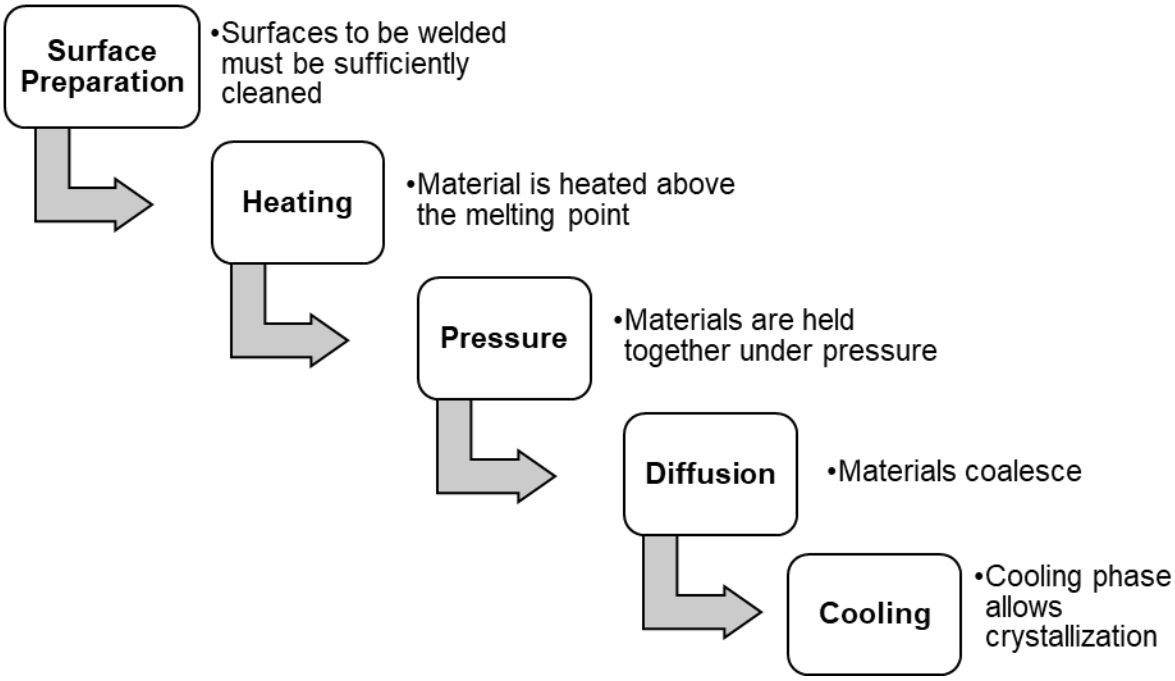

Figure 4: Five general phases of thermoplastic welding processes

All welding methods consist of the phases: surface preparation, heating, pressure, diffusion, and cooling. Although their phases are similar, the heating methods vary significantly depending on the material to be joined. Some materials can be welded with almost any welding method, while other materials are very limited on which methods can be used. The characteristics of the material such as the melting point and the molecular properties of a material determine which welding methods are applicable. PTFE is more difficult to weld than most thermoplastics due its characteristics as discussed in the properties section earlier in this paper. The following table from *Thermoplastics and Thermoplastic Composites: Thermoplastic Processing* displays common thermoplastic materials and which type of welding is applicable for each material (Biron 1980).

Table 1: Common thermoplastic materials and their applicability to welding methods (Biron, 1980)

	Welding			Adhesive bonding
	Thermal	HF	Ultrasound	
ABS	Good	Fair to good	Good	Good
Cellulosics	Good	Fair to good	Fair	Good
PA	Good	Fair to good	Good	Good
PC	Good		Good	Good
HDPE	Good	Unsatisfactory	Fair	Fair
LDPE	Good	Unsatisfactory	Fair	Fair
PET, PBT	Fair	Fair to poor	Good	Fair
PTFE	Fair	Unsatisfactory		Difficult
PMMA	Good	Fair	Good	Good
POM	Good		Good	Fair
PP	Good	Unsatisfactory	Good	Fair
PPE	Fair		Fair	Good
PS	Good	Unsatisfactory	Good	Good
EPS	Good			Good
TPU	Good	Fair		Good
Soft PVC	Fair	Good	Fair	Fair to good
PVC	Fair	Good	Good	Good
PVDC	Good	Fair to good		
PSU		Unsatisfactory	Good	
Foamed PVC		Good		

As shown in Table 1, PTFE is not very applicable to the most common heating methods. Represented in the table are three types of welding methods and adhesive bonding. The three types of welding listed in Table 1 are thermal, HF (High Frequency), and Ultrasound. Thermal represents the external heating methods. High Frequency, or Radio Frequency (RF), represents the electromagnetic internal heating methods, and Ultrasound represents the internal mechanical heating. The only method that is applicable to PTFE is the thermal welding method, and it is only listed as “fair”. The only common welding method that is applicable to PTFE is hot plate welding. This method is similar to the current welding method with the exception to the placement of the heaters. Hot plate welding has the greatest applicability to PTFE and will be explained in detail below.

2.2.2.1 Hot Plate Welding

2.2.2.1.1 Overview

Hot plate, or hot tool welding is arguably the most common form of thermoplastic welding. The method uses a hot tool, or platen that heats each face of the plastic parts to be joined. Once

the faces of the parts are melted, the hot plate is quickly removed, and the faces of the parts are pressed together and held under pressure while cooling. The *Handbook of Plastics Joining* provides the below figure for the way that hot plate welding works (Troughton, 2008).

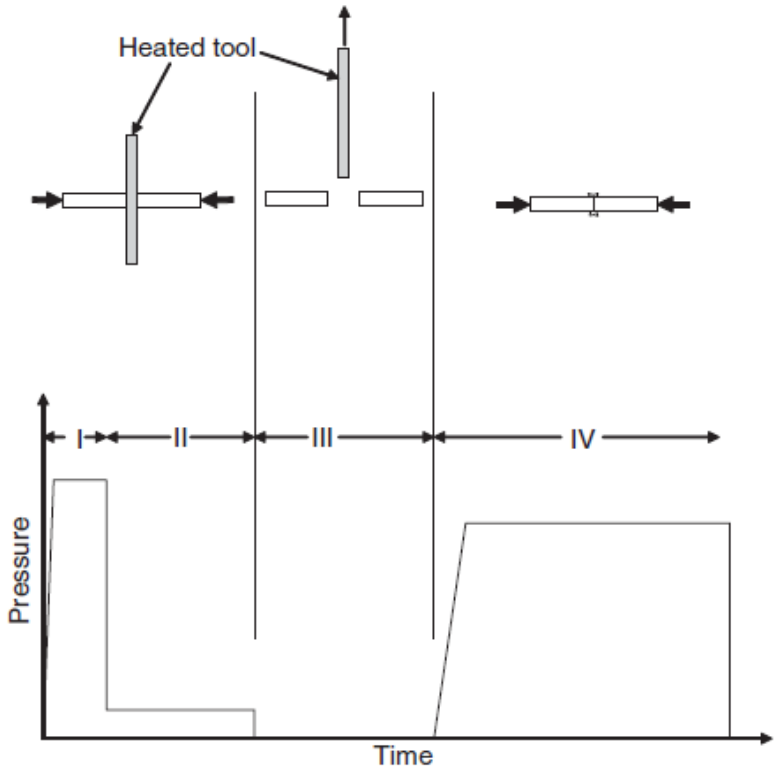

Figure 5: Phases of hot plate welding method (Troughton, 2008)

As shown in Figure 5, the plastic is held under pressure during both the heating and cooling phases. During heating, the parts are held under pressure to ensure that the plastic begins to flow and that the surface irregularities are gone. Once the plastic begins to flow after reaching melting temperature, the heated tool is removed and the parts are joined under pressure. The advantages of hot plate welding are that it is very economical and versatile. Hot plate welding is suitable for almost any thermoplastic and can join two different materials of thermoplastics. Hot plate welding however relies on very quick heating generally to get the surfaces of the plastic to their melting point. It is typically best for softer semi-crystalline plastics and is not applicable for high molecular weight plastics such as nylon or PTFE (Troughton, 2008). This is because hot plate welding relies on thermal conductivity to get the plastic to the molten state. PTFE has poor thermal conductivity and a high molecular weight. Due to the molecular weight, it does not flow when heated above

the melting point. Also, due to the low thermal conductivity, it does not heat up quickly, but rather will degrade the plastic if heated too rapidly. The applicability of a fluoropolymer is related to the material's rheology (Ebnesajjad, 2015). A high rheology or melt viscosity reduces the number of methods that are applicable to the material (Ajroldi, 1970). Ajroldi goes on to explain that the least amount of methods are applicable to PTFE.

2.2.2.1.2 Parameters

The parameters that are important for hot plate welding, and most welding methods in general are the following: temperature, pressure, and time. The temperature of the plastic at the butt joint must reach a temperature high enough above the melting point of the plastic. The *Handbook of Plastics Joining* explains that the hot plate temperature should be in the range of 30°C - 100°C above the melting point of the material (Troughton, 2008). For low viscosity materials, sticking to the hot plate can sometimes be an issue which then causes stringing of the material to the plate. This can then lead to issues with future welds because the heated tool is less effective. High temperature welding can combat this in some way. High temperature hot plate welding uses temperatures between 300°C and 400°C (Ebnesajjad, 2015). This however is for common thermoplastics. These temperatures are hardly above the melting point for PTFE.

The pressure of the weld is also an important parameter to hot plate welding. The pieces to be welded are generally held under pressure during both the heating and cooling phases of the weld process. When held under pressure during heating, this is called the matching phase. This phase ensures the surface irregularities are melted off the faces to be welded, and that the molten layer becomes smooth. Welded plastic parts are also held under pressure during the cooling phase of the weld. This ensures proper fusion of the two interfaces to be welded and creates the "polymeric chain entanglements" that provide the material with its mechanical strength characteristics. The *Handbook of Plastics Joining* explains that when cooling under pressure, the molten material flows outward and creates a flash (Troughton, 2008). The pressure during cooling allows the material to be properly joined so that it coalesces and gets rid of any voids or air pockets. Troughton goes on to say that it is imperative to hold the molten material under pressure because during this phase is when the final molecular structure is formed and when the residual stresses occur (Troughton, 2008). Holding the material under pressure thus prevents warpage in the material.

2.2.2.1.3 Applicability to PTFE

Unfortunately, PTFE is not listed as a material that is easily joined through the method of hot plate welding. *Fluoroplastics* lists PTFE as applicable to hot plate welding "under certain conditions" (Ebnesajjad, 2015). Biron categorizes the weldability of PTFE through hot plate welding as fair (Biron, 1980). It is more common to see PTFE listed as the material for the non-stick coating on the heater plates for hot plate welding methods. Numerous sources list PTFE or Teflon (Dupont's trade name for PTFE) as the coating used on the hot plate. This prevents the other thermoplastics being welded from sticking to the plate due to its low friction coefficient. PTFE is not used however as a non-stick coating for high temperature hot plate welding. This is because the higher temperatures will degrade the PTFE material.

Hot plate welding also generally has extremely fast cycle times. Grewell and Benatar explain that typical cycle times range from 30-90 seconds and as long as 30 minutes for larger parts (Grewell et al. 2007). This however is much faster than the 10-hour cycle times of the current PTFE welding process. Thus, hot plate welding seemed to be an applicable solution for PTFE, but the heating rate must be slower due to the low thermal conductivity of PTFE. If too high of a temperature is used, the material on the face will begin to degrade before the material in the middle has reached a proper welding temperature. This must be kept in mind when trying to reduce the cycle time with any method but especially with hot plate welding because it is generally used for plastics that are easily melted.

Many sources also discuss the use of PFA with PTFE when welding. This material is introduced as a film layer between the two PTFE layers to be welded. This material has very similar strength characteristics to PTFE but has a higher weldability. The current welding process uses this material as a film between the two PTFE bars of material to be joined. Because of the melting point of PTFE, the weld temperature required would be much higher than that of common thermoplastics with lower melting temperatures. As discussed in many articles about hot plate welding, high temperatures in the method of hot plate welding can potentially cause the materials to stick to the hot plate between the materials, causing poor welds. In *Fluoroplastics*, it is also discussed that high heating rates do not accelerate the process when there is a low conductivity such as with PTFE at typically 0.25 W/m-K (Ebnesajjad, 2015). However, there are limited sources which show that PTFE can be welded through a hot plate method. Thus, for now it is

considered that hot plate welding is an applicable method under certain conditions and with special design considerations.

2.2.3 Cooling

An important part of thermal welding processes is the cooling phase. The rate of cooling greatly affects the material properties of the weld. Thermal stresses, or residual stresses are a result of contractions due to the hot and cold regions of the weld. Additionally, it was shown that for a hot plate welding method, the residual stresses are lower with a higher plate temperature and a longer heating time (Sojiphan et al., 2009). Studies have also been done showing that a longer cooling time increases PTFE's crystallinity and thus its wear resistance (Hu et al., 1983). Price et al. showed in their study that the cooling rate of PTFE affects not only the crystallization but also the thermal conductivity (Price, 2002). With a slow cooling rate of 1 °C/min, the crystallinity and thermal conductivity were 76% and 0.298 W/m-K at 232°C; while at a fast cooling rate of 40°C, the crystallinity decreased to 61% and the thermal conductivity to 0.279 W/m-K at 232°C (Price, 2002). Therefore, the cooling rate has a substantial effect on the crystallinity of PTFE. The crystallinity of PTFE then affects the thermal conductivity and wear resistance among other properties. The current process has an established cooling rate for the desired material properties, and therefore the cooling rate of the PTFE was not changed.

2.2.4 Comparison of Welding Methods for PTFE

In general, common thermoplastic welding methods are not meant for materials such as PTFE. They are designed for quick melting, low viscosity materials that flow when melted. PTFE is not easily melted and does not flow when melted but rather becomes "rubbery". Thus, most of the common methods are not applicable. In fact, in "Microwave/RF Applicators and Probes" by Mehrdad Mehdizadeh, there is mention of using PTFE as a dielectric buffer layer while welding other thermoplastics (Mehdizadeh, 2015). PTFE has also been used as the vessel for other molten thermoplastics to flow through (Soundarrajan, 2014). In some hot plate welding tooling, the hot plate is coated with PTFE (Bucknall et al., 1980). Thus, it is resilient enough to withstand the welding of other thermoplastic materials. Friction methods are also difficult with PTFE as it has the lowest coefficient of friction of most materials. Other manufacturing locations have done work with welding thermoplastic materials, but none are directly applicable. One location uses a

welding machine for PEEK material. PEEK is a high temperature plastic such as PTFE, but it melts and flows better than PTFE, thus, it lends itself to easier welding. Another manufacturing location uses induction welding for PTFE with carbon fiber additives. However, this requires an implant material to be placed between the two pieces of material. Also, this material compound has carbon fiber fillers present that allow it to be applicable to induction welding. Other material compounds that have different or no fillers such as virgin PTFE, or glass would not be applicable to this method. The type of welding that is the most applicable to PTFE is by external thermal means. The book, *Thermoplastics and Thermoplastic Composites* in chapter 5 lists PTFE as "Unsatisfactory" for HF or RF welding, NA for ultrasonic welding, and "Fair" for thermal welding (Biron, 2018). This agrees with other sources that have investigated the topic of welding PTFE. Some sources describe using a hot plate method for welding PTFE; however, the part to be welded was a tube with a small wall size. No sources indicated attempting to weld a bar of PTFE as thick as the rings joined together in the application in question. Thus, there are no clear best practices for a sound design of a PTFE welding machine.

2.2.5 Current Method for Welding PTFE

Currently, a manufacturer of PTFE seals uses a thermal welding method to join the two pieces of PTFE. There are six welding machines that join the pieces of PTFE. Figure 6 below shows the fixture that is used for welding the pieces of PTFE material.

Figure 6: Picture of welding fixture

Out of the six total welders at a PTFE seal manufacturer, four are the pictured style. The two other welders are of different styles, one older and one newer. However, because the pictured welder is the standard, this style was used as the standard for the purposes of this project. A diagram of the cross section of the welding process along with process steps are outlined below in Figure 7.

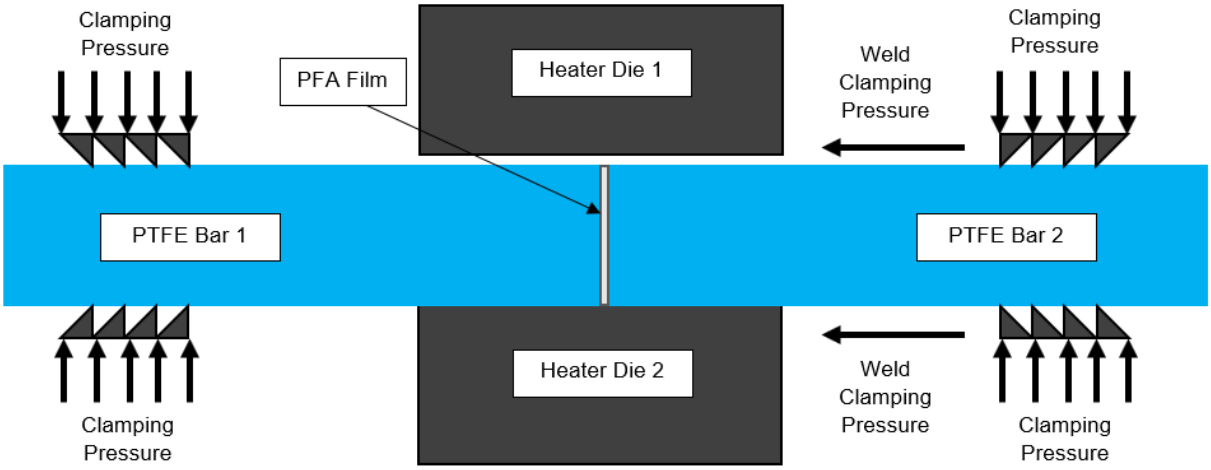

Figure 7: Cross section view of welding process

Figure 7 above shows a cross section view of the welding process used to weld large diameter PTFE rings. As shown, two pieces of PTFE are joined together through the welding process. Below are abbreviated steps for the welding process:

1. Each end of the PTFE bars to be welded is cut.
2. The heater dies are cleaned and lined with Aluminum Foil.
3. PTFE Bar 1 is loaded into the stationary clamp and into the heater.
4. PTFE Bar 1 is clamped with a pneumatic cylinder to hold it in place
5. PTFE Bar 1 and 2 faces are cleaned to remove any oils or dirt from the surface
6. PTFE Bar 2 is placed into the heater dies with a small gap in between the two pieces of material (approximately 1/8”).
7. Placed between the gap is P.F.A. Fluorocarbon Virgin Film.
8. The PTFE sides 1 and 2 are then clamped together under low pressure.
9. The weld cycle is then initiated.

The heater dies are located above and below the PTFE pieces and are made of naval brass material. They also surround the sides of the material; however, it is not shown in Figure 7 for clarity. Figure 8 below shows an assembly view of the heater dies without the PTFE material inserted into each end.

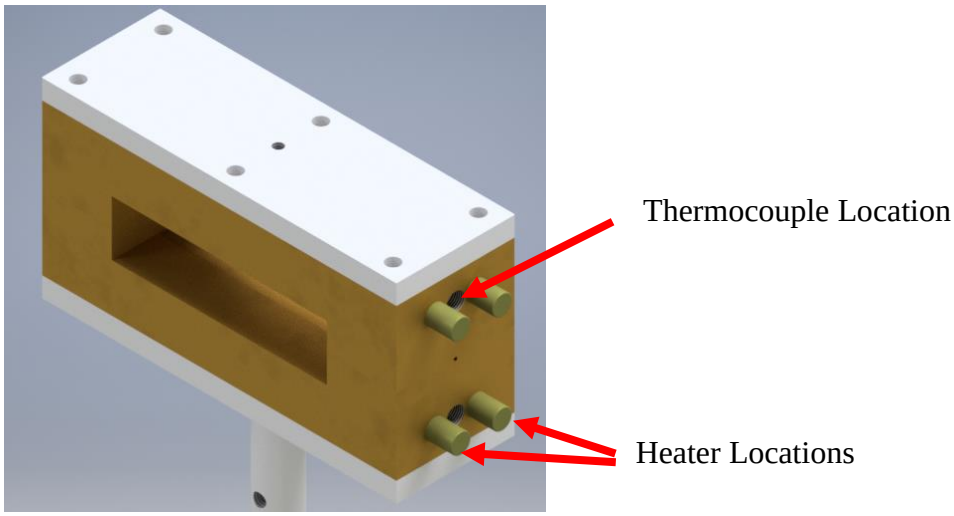

Figure 8: Assembly view of heater dies

In each heater die, there are two cartridge heaters and one thermocouple in between the heater dies. The thermocouples are used as feedback for the controller. Based on this temperature feedback, the controller determines how much power to send to the cartridge heaters according to the selected welding cycle.

There are different welding cycles based on the different material compounds that can be welded. Most materials use the same cycle while other specific materials have their own cycle. For this research, the most common welding cycle was used for modeling and simulation as it is applicable to the most materials and the most frequently used weld cycle. All of the weld cycles that are used for the welders consist of a ramp up time, a hold time, and then two cool down phases. The times and temperatures for each phase vary between programs. During the ramp up phase, the temperature is increased from ambient to the desired maximum temperature. In the hold phase, the desired maximum temperature is held constant. During the cool down phase, there are two phases in which the material cools to an intermediate temperature and then to ambient temperature at different cooling rates. Figure 9 below shows the temperature profile used for the modeling in this project. The times and temperatures are left out for proprietary purposes.

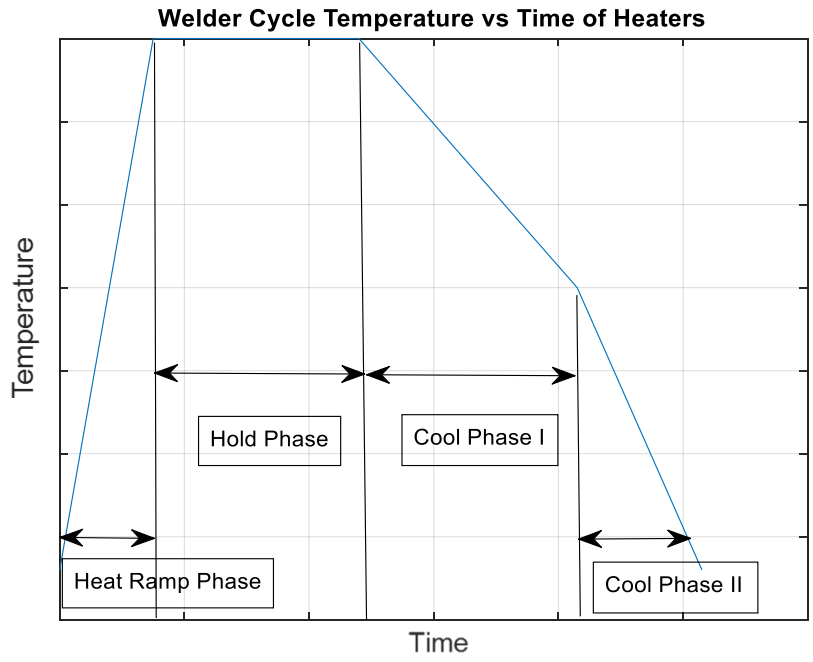

Figure 9: Welding cycle currently used to join PTFE

On the Y axis of this plot is the desired temperature of the heater dies throughout the weld cycle. This temperature is what the controller is trying to regulate throughout the weld process. The controller turns the cartridge heaters on and off to keep the dies at the desired temperature based on feedback from the thermocouples in the dies between the heaters. The heaters do not have their own regulation on the amount of power that they output; thus, the power is adjusted through pulse width modulation to control the percentage of power.

In the specified program, the heater dies are heated during the ramp up phase. Then, they are held at a constant temperature. During both phases, the clamping pressure holding the pieces of material together is a constant low pressure. Once both phases are complete, the clamping pressure is increased. Simultaneously, the slow cool down phase begins. There are two cool down phases at different rates as can be seen in the plot of the heating and cooling phase. Due to the material properties in which PTFE cools, the cooling phases cannot be changed. Thus, for the scope of this project, the focus will be on the first two phases of the heating cycle.

The heating phases of the PTFE during the welding process include a ramp phase and a temperature holding phase. These phases describe how the heater dies are heating up the PTFE material. The overall goal of this project is to research the potential to reduce the cycle time of the

overall welding process. Because the cool down phases will not be changed in order to maintain the desirable crystallinity of the material, the modeling and simulation will aim to model these first heating phases. This research will determine if it is possible to reduce the cycle time by reducing the heating time of the material to be welded.

2.2.6 Critical Factors

As previously mentioned, the cooling phases of the welding cycle will not be examined due to the effect that the cooling rate has on the crystallinity of the material. Ting-Yung Hu and Norman Eiss discuss how the crystallization of PTFE is directly related to the cooling rate (Hu et al. 1983). The authors also discuss that the mechanical properties increase with decreasing crystallinity. Crystallinity and the corresponding material properties are more dependent on the cooling rate than the heating rate. Thus, reducing the time for the heating phase would not have a negative effect on the material properties of the welded PTFE. Another critical part of welding PTFE is to make sure that the material is well above the melting point (Ebnesajjad, 2015). However, PTFE can begin to degrade if it is held for too long at a temperature high above the melting point. Thus, this must be kept in mind when trying to increase the rate at which the material is heated. The time that it takes to reach a suitable welding temperature is dependent on the size of the part due to PTFE's low thermal conductivity. Thus, the part size will be a constraint on how fast the material can be heated. Another important part of welding any thermoplastic is to hold the pieces together under pressure once the welding temperature is reached throughout the material. This allows the material to coalesce and remove any voids or air gaps that would prevent the material from having a solid weld (Ebnesajjad, 2015). This welding process has been used for years; however, there are still instances where welds fail when tested. The welds generally fail in the center of the material when they do. This suggests that the material gets hot enough around the edges, but not hot enough in the center so that the material can coalesce properly. Consequently, any design changes that are suggested because of this project to reduce the cycle time will also aim to ensure that a weld is of desirable quality all the way through the material.

2.2.7 Modeling

The modeling of welding processes has been done, but not for PTFE welding processes. A hot plate welding process for polycarbonate has been analyzed for both a thermal and residual

stress analysis with temperature dependent properties (Sojiphan et al. 2009). From their results, the heating time had a more significant effect on the temperature distribution than the heating temperature. However, these tests were only for short, hot plate welding cycles. Zhu et al. discussed a welding process simulation for metals but not for thermoplastics (Zhu et al., 2002). They also discussed that it is difficult to obtain temperature dependent material property data at elevated temperatures, to which they employed a different method. In their simulation, tests were done to compare the effects of varying temperature dependent properties vs constant properties. Their tests showed that constant room temperature values could be used for specific heat, thermal conductivity, and density (Zhu et al. 2002). This however was for aluminum and there have not been any studies as to if this same method is applicable to PTFE. It has also been shown for 2-D transient calculations that reducing the time step improves the accuracy of the calculations more significantly than increasing the mesh size (Thomas et al., 1984). There has been work done on the simulation of welding processes, but not for an application like this research. Thus, a MATLAB model was developed for this process to simulate the 2-D transient heat conduction in the PTFE.

3. MODELING AND SIMULATION

To develop a method for improving the design of the welding apparatus, the current method must be fully understood. Thus, the focus of this project was to develop a model that could simulate the current process accurately enough to see if the weld cycle time could be reduced by changing the inputs to the current design. A model was built using MATLAB to calculate and display the results of a temperature distribution of the current process. The following sections will discuss the building of the model, the results, the assumptions made, and how this model can be used to employ design changes.

3.1 Description of Problem

The analyzed welding process is an adapted welding process that is different from most thermoplastic welding procedures due to the nature of PTFE's material properties. It resembles a sintering cycle more so than a welding cycle because of the long cycle times. Depending on the size of the large diameter PTFE ring desired, a ring may consist of anywhere from one to 4 or more welds in each ring. With a total cycle time of over 10 hours for each weld, this is a huge amount of time invested in a welded ring. Due to the manufacturing environment, a much shorter weld time would save the company time and therefore money on each weld. The goal was to determine if the cycle times could be reduced with the current process, and if not, what design changes would reduce the overall time. Another concern is the quality of the weld produced. Currently, each weld on a welded ring is tested on an Instron tensile test machine to verify that the weld is adequate. The location of the tested weld is at the edge of the material however. It is not uncommon for there to be a weld that is acceptable on the edges, but bad in the center. Bad in this case refers to material in the center of the two pieces that did not properly join. When a weld fails in this way, it suggests that the material is getting hot enough around the edges, but not hot enough in the center. Thus, it was of interest to know the temperature distribution at the face of the piece of PTFE to be welded. The model created for this project calculates the temperature distribution at the face of the PTFE to be welded after a given input amount of time. For the results of this project, the first 90 minutes, or the ramp time of the welding cycle was analyzed in detail. As mentioned, a

MATLAB model was constructed to perform a numerical simulation of the current process using the finite difference method.

3.2 Assumptions Made

3.2.1 Modes of Heat Transfer

The accurate modeling of this welding process is an extremely complex heat transfer model. Therefore, this model uses assumptions to simplify the calculations based on the goals of this project. This project was designed to analyze the current process to determine if design changes could be made. The main goal of this project was to build a model that accurately reflected the results of the current operation which could then be used for design improvement analysis. Thus, it was not of interest to determine exactly the modes of heat transfer to the material, but rather to have a model that predicted accurate results for the current process. In the actual process, heat is transferred from the heater dies to the material by means of conduction, convection, and radiation. Therefore, there are losses from each of these modes of heat transfer. Rather than determining each of these modes of heat transfer individually, the heat flux on the boundaries was assumed to be an equivalent heat transfer taking these modes and losses into account. Figure 10 below shows the terms of the heat transferred to and from the material.

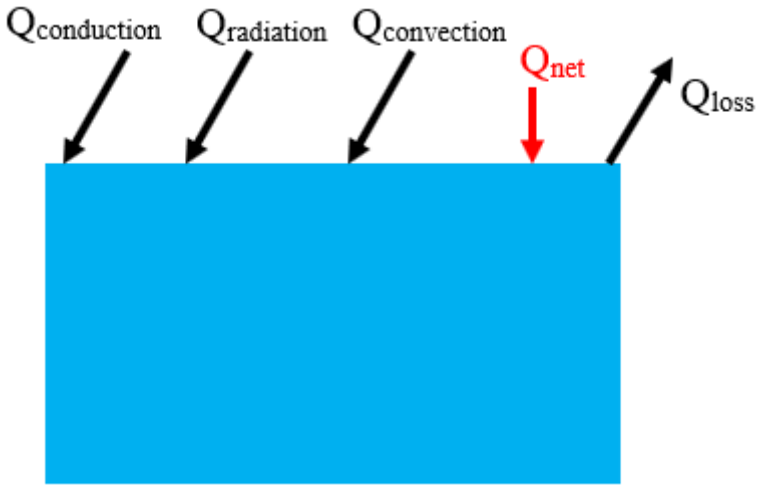

Figure 10: Heat loss terms taken into account for Q_{net} on the PTFE material

Because there is an initial air gap between the top of the PTFE material and the heater die, there is convection and radiation between the PTFE and the heater dies. There is also heat loss from the PTFE and the heater dies. This heat loss would change as the temperature of the material is changing. Thus, the resultant heat transferred to the material was captured as Q_{net}. Therefore, in the MATLAB model, there is one heat flux value on the boundaries that takes these various heat loss terms into account for simplicity. This heat flux was calibrated based on results which will be discussed in the Verification & Validation section.

3.2.2 2-D Numerical Solution

The welding process performed by the manufacturer of PTFE seals in question is a transient 3-D heat conduction problem. Although the heat conduction happens in 3-D in the material, the only part of interest in the material is at the joining face of the weld between the two pieces of PTFE. Hence, the model that was created calculates the temperature distribution at the face of the pieces of material to be welded. Though heat transfers to the material in the direction perpendicular to the face of the weld, it was assumed that this amount was insignificant compared to the other directions and thus could be modeled as a 2-D solution. It was also assumed that the 2-D solution is constant for the section of material in the heater dies. Heat will be diffused throughout some of the material in the Z direction in Figure 11; however, it is assumed that the heaters cover a large enough section so that the problem can be treated as 2-D for a small section of the material. Thus, the MATLAB model uses 2-D numerical heat conduction calculations to determine the temperature profile in the face of the material at the joining point. Due to symmetry, the material face can be divided into symmetric halves. The material could likely be divided symmetrically again along its centerline parallel with the x-axis, however, at the time of building this model, it was unclear if the top and bottom faces had the same boundary conditions. Therefore, the MATLAB model was built to model one half of the face of the PTFE bar that is in the welder heater dies. Figure 11 shows the area of the material used in the simulation.

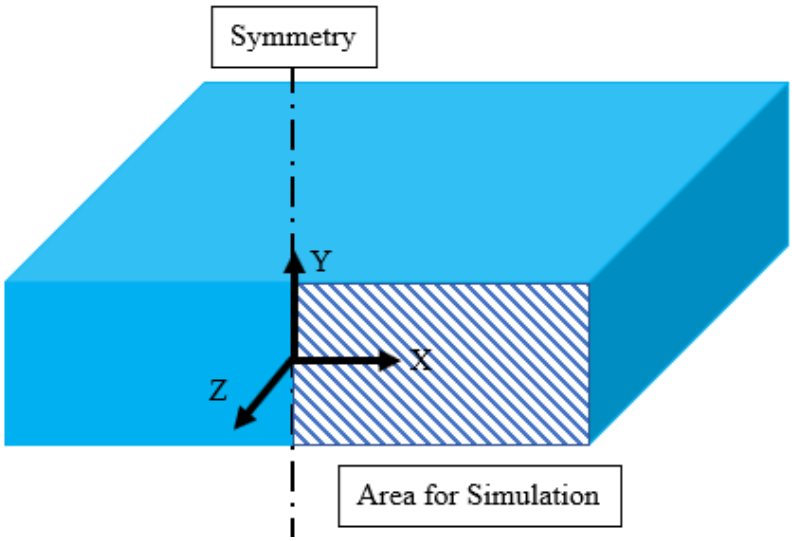

Figure 11: Simulation area for the MATLAB model to calculate the 2-D transient temperature distribution

Because of its simple rectangular shape, the material is symmetric along both the X and Y axes, but the code was built only using the symmetry along the Y axis. Accordingly, the results from the MATLAB model show the temperature distribution for the cross hatched area shown above. The next section will discuss the determination of the boundary conditions.

3.2.3 Stability

The Fourier Number is an important measure of the stability of transient heat transfer. Based on the boundary equations for a 2-D transient finite difference method, the Fourier Number should not exceed $F_o = 1/4$ for stability (Mills, 1992). For this model, the goal was to keep the Fourier Number at $F_o < 0.1$. This was assumed to be well enough below the stability criterion to ensure that the calculations were stable and accurate. At each new time step when the Fourier Number is updated, the MATLAB model checks for stability and gives an alarm and stops the program if it is greater than 0.1. In this model, the Fourier number changes at each time step because the material properties are temperature dependent. In the code, the Fourier Number variable contains a matrix of values with a Fourier Number at each node. The stability check of the Fourier Number checks the maximum value in that matrix and gives an alarm if the maximum value is above 0.1. For 2-D transient heat conduction, the equation for the Fourier Number is

$$F_o = \frac{\alpha \Delta t}{\Delta x^2} \qquad (1)$$

The Fourier Number is also dependent on both the time step for the transient response and the distance between the nodes, Δx. Consequently, if the Fourier Number was well below the stability criterion, it was assumed that the time step Δt and distance Δx were also small enough.

3.3 Material Properties

An important factor in the building of this model was the material properties used for the calculations. Because this process raises the temperature of the PTFE above the melting point, temperature varying material properties were used for the calculations. The key material properties used in the 2-D transient heat conduction calculation were density, specific heat, and the thermal conductivity of PTFE. The values of thermal conductivity and density for virgin PTFE were gathered from data from the company's MTL. Initially, the MTL had limited data on temperature dependent thermal conductivity. A test request was placed to have the thermal conductivity of virgin PTFE tested at various increasing temperatures. After testing, it was unclear what the transient behavior of thermal conductivity was. Though more extensive testing and verification is required, the recommended data to be used is presented in Figure 12.

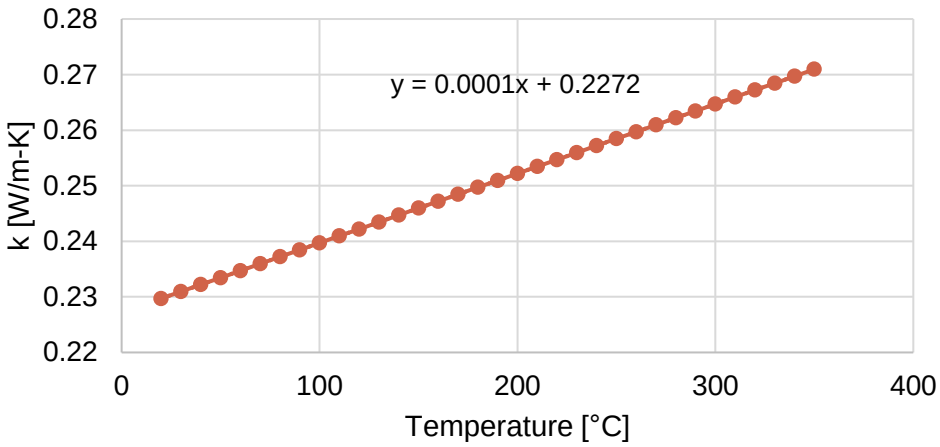

Figure 12: Transient response of the thermal conductivity of PTFE from ambient to above the melting point

The thermal conductivity of PTFE remains fairly constant at increased temperatures, only gradually linearly increasing above the melting point. At ambient temperature, 23°C, the thermal

conductivity is 0.23 W/m-K and increases to around 0.27 W/m-K at 350°C which is above the melting point.

For the temperature varying specific heat, the test lab did not have data other than at ambient temperature. Instead, data was gathered from *The Thermodynamic Properties of Polytetrafluoroethylene* for crystalline PTFE from 0 to 700 K (Lau et al., 1984). PTFE melts at 605 K, so this data provided the specific heat capacity of PTFE above the melting point. Lau et al. give a summary of recommended material properties for PTFE based on tests of PTFE with varying crystallinity. PTFE is a crystalline polymer with typically 93-98% crystallinity (Pethrick, 1989). The research conducted for this article investigated various thermal properties of PTFE; however, the property of interest from this article was the heat capacity for crystalline PTFE. Table II in the article gives a recommended range of the heat capacity summarized from previous studies and the authors additions and is shown in the Appendix in Figure 56 (Lau et al, 1984). The data is presented in units of J/mol-K in the article and is thus molar heat capacity. To convert the molar heat capacity values to mass based specific heat, the given value was divided by the molar mass of PTFE, 0.100015 kg. This was calculated using the chemical formula for PTFE, C_2F_4 and the corresponding atomic masses. The table showing the calculated specific heat from the molar specific heat capacity is also shown in the Appendix in Table 10. The chart below shows the summarized data plotted with the corresponding fitted equation used for the temperature dependent specific heat.

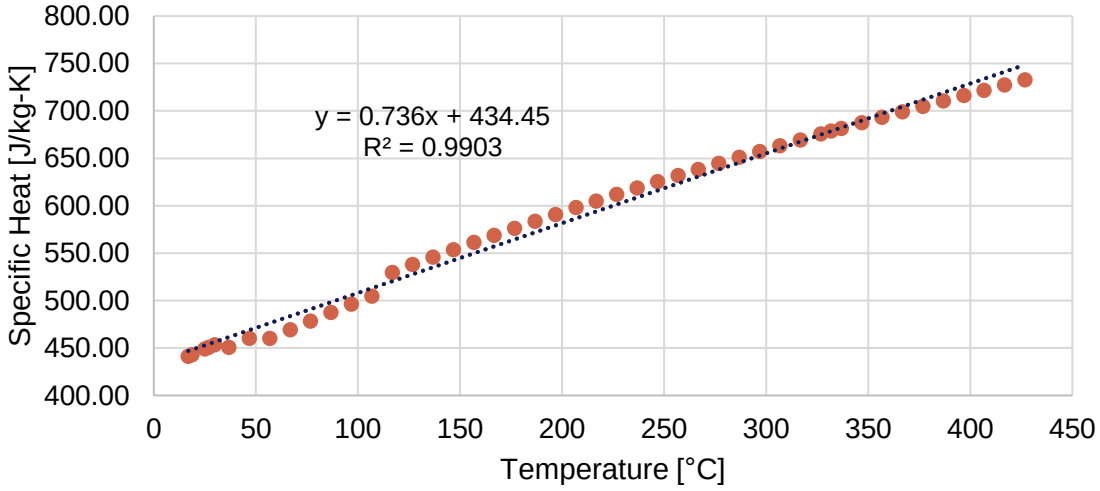

Figure 13: Transient response of specific heat for crystalline PTFE based on data from (Lau et al., 1984)

The plot shows that the relationship between the specific heat vs temperature is a mostly linear relationship. The linear fitted equation has an R^2 value of 0.99 and thus accounts for 99% of the variability in the data. This shows that the fitted equation can be confidently used to model the specific heat data.

The next property that was used in the MATLAB model was the density of PTFE. The MTL only had data for the density at ambient temperature; however, there was data for the dimensional change of PTFE at increasing temperature. The figure summarizing this data is attached in the Appendix in Figure 57. The thermal expansion and dimensional change are given at increasing temperatures. The temperature dependent density was then derived from this data. Assuming a linear thermal expansion in all dimensions, the volumetric change was calculated. The mass and the volume used for the calculations was the amount of material that is in the heater dies. The dimensions for this amount of material are shown below in Table 2.

Table 2: Constants used the volumetric change calculation

Width of bar [m]	0.0978
Height of bar [m]	0.0229
Depth of bar [m]	0.0579
initial volume [m³]	1.29E-04
Ambient Temperature	73.4
initial density [g/cm³]	3.07 per data at 23°C
initial density [kg/m³]	3070
mass [kg]	0.2796

After calculating the mass and initial volume of the material in the heater dies, the final volume could be calculated. The volume at each temperature was calculated using thermal expansion data and assuming linear change in all dimensions. Rearranging the relationship for volumetric thermal expansion yields

$$\frac{\Delta V}{V_o} = 3\alpha\Delta T \tag{2}$$

$$V = V_o(1 + 3\alpha(T - T_o)) \tag{3}$$

from which the density was calculated

$$\rho = m/V \tag{4}$$

The temperature dependent density for PTFE based on the thermal expansion data is presented in Figure 14.

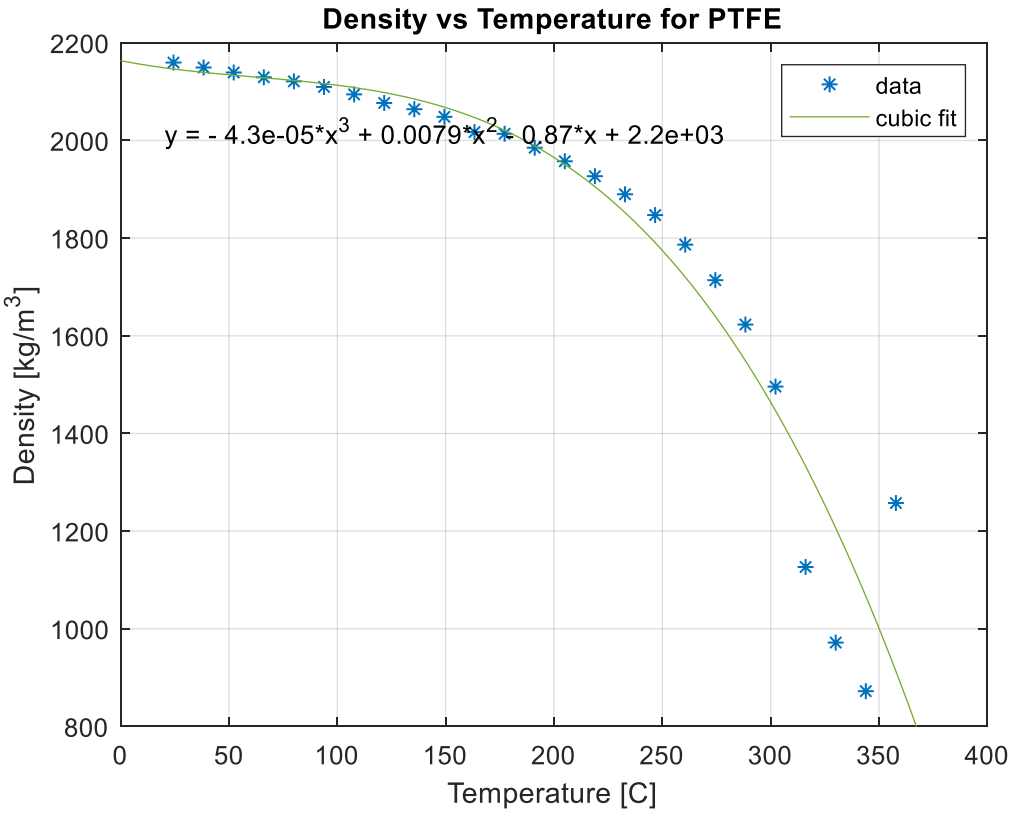

Figure 14: Transient response of the density of virgin PTFE based on thermal expansion data from ambient temperature to above the melting point

The temperature dependent density varies more at elevated temperatures around PTFE's melting point. For this model, the plot was fitted with a cubic regression line. A regression analysis was performed in Minitab 18 which found that the R^2 adjusted value was about 92%. This means that 92% of the variability was accounted for and while it is acceptable, more information would need to be acquired to confirm that it is an accurate model. The displayed equation was used in the model to calculate the density at the corresponding temperature. More investigation should be done on the accuracy of the density curve and the expansion behavior of PTFE around the melting point. The density, thermal conductivity, and specific heat were important for this model because they are used in calculating the Fourier number, an important factor in transient heat transfer stability.

3.4 Boundary Conditions

3.4.1 Modeling the Heat Flux

Once the area for the simulation was determined, the boundary conditions on each side were determined. In order to do this, the tooling for the welding process was further examined. In each of the top and bottom heater dies, there are thermocouples placed in the center of the block that can be seen in Figure 15 and Figure 16.

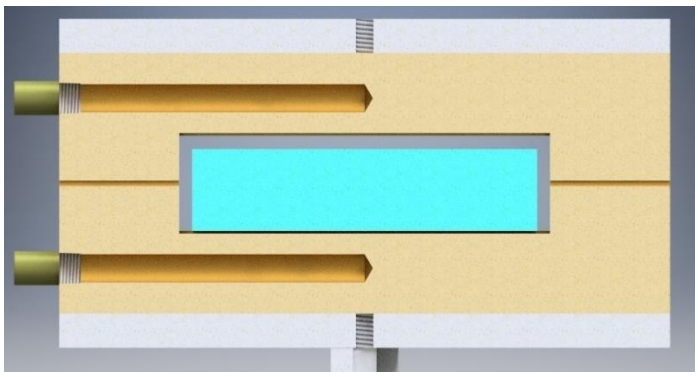

Figure 15: Cross sectional view showing the location of the thermocouples in the heater dies

As shown above, the thermocouples are placed to read the temperature in the center of the heater dies. The thermocouples are also placed in the center of the dies in between the two cartridge heaters in each block. Figure 16 below shows the side view of the heater dies showing the locations of the thermocouples and cartridge heaters.

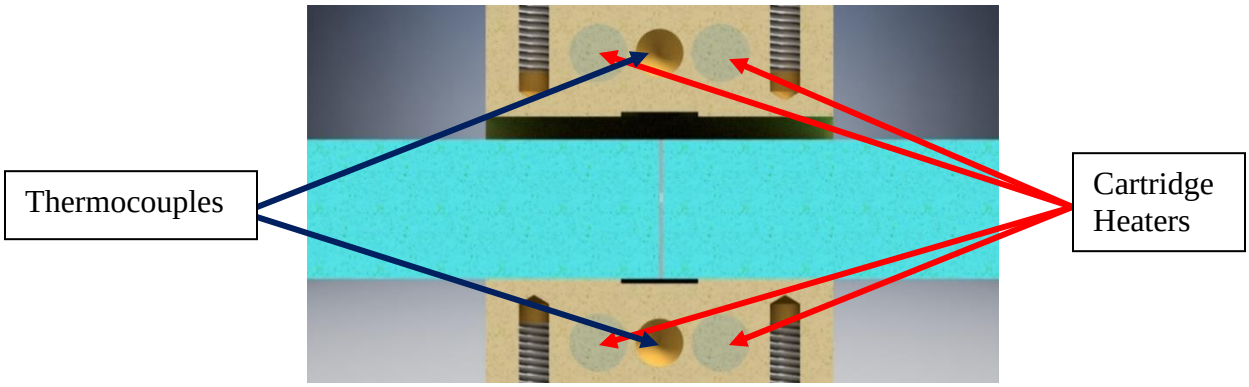

Figure 16: Location of the thermocouples and cartridge heaters within the heater dies

As can be seen in Figure 16, there are two cartridge heaters in both the top and bottom heater dies. Also, there is one thermocouple in each die, located between the heaters. In the controller, the heater dies are labeled as zone 1 and zone 2. The controller uses the temperature feedback from these thermocouples to govern the amount of power that goes to the cartridge heaters. The cartridge heaters do not have power control, so when they are on, they are on full power. The technique that is used to control the amount of heat given from the heaters is controlled using pulse width modulation (PWM). In pulse width modulation, there are intervals where the power is turned on and off with a percentage to simulate an average value. Figure 17 shows a basic plot of voltage versus time using pulse width modulation.

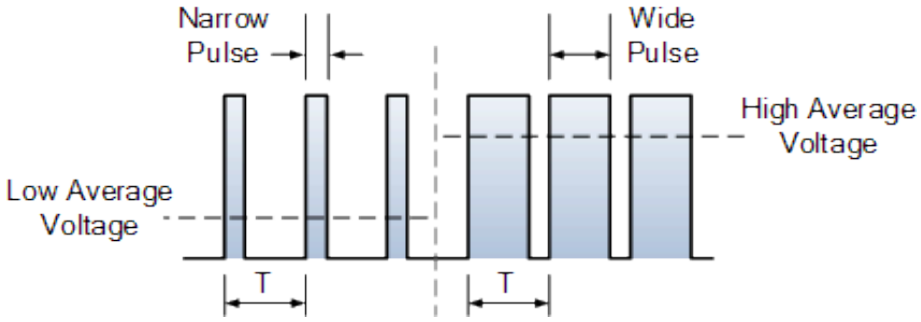

Figure 17: Pulse width modulation used by the cartridge heaters: short and long pulse times and the corresponding average voltage PWM ("Electronics Tutorials")
https://www.electronics-tutorials.ws/blog/pulse-width-modulation.html

To achieve the desired average power or voltage value, the percentage of power or voltage is adjusted. When this power percentage is adjusted, the time in which the heaters are on is adjusted. For example, when the power percentage increases, a wider pulse is used so that the heaters stay on longer. Contrarily, for less power, the pulse time decreases. On the controller, the power is given as a percentage for the amount of power going to each of the cartridge heaters as shown in Figure 18 below.

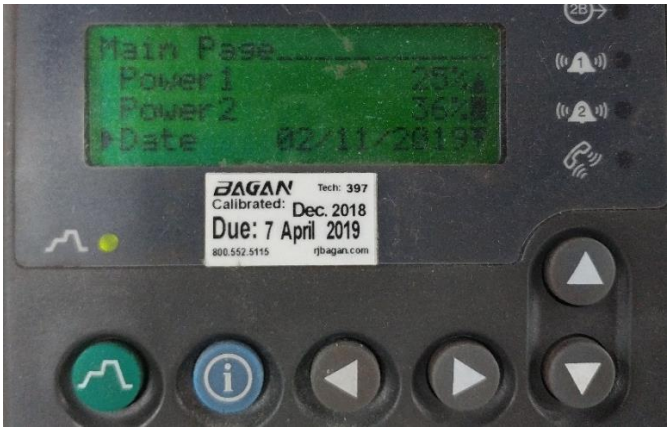

Figure 18: Welder cycle controller displaying the power percentage of each heater die

This shows the power level for each of the heater dies at a short time after the cycle was started. In the controller, there is a program which specifies a temperature profile for the heaters to follow. The controller uses feedback from the thermocouples along with the target temperature in the program to govern the amount of power going into each of the heaters. The amount of power going into the heaters was modeled as a heat flux boundary condition in MATLAB. As mentioned, the exact heat flux going into the material was unknown because some of the heat input into the heaters is lost to the surroundings. The heat flux boundary was tuned based on validation data.

A heat flux boundary was used for the top, bottom, and right edges, and an adiabatic boundary was used for the left edge due to symmetry. Figure 19 shows the boundary conditions that were used for the simulation area of the MATLAB model.

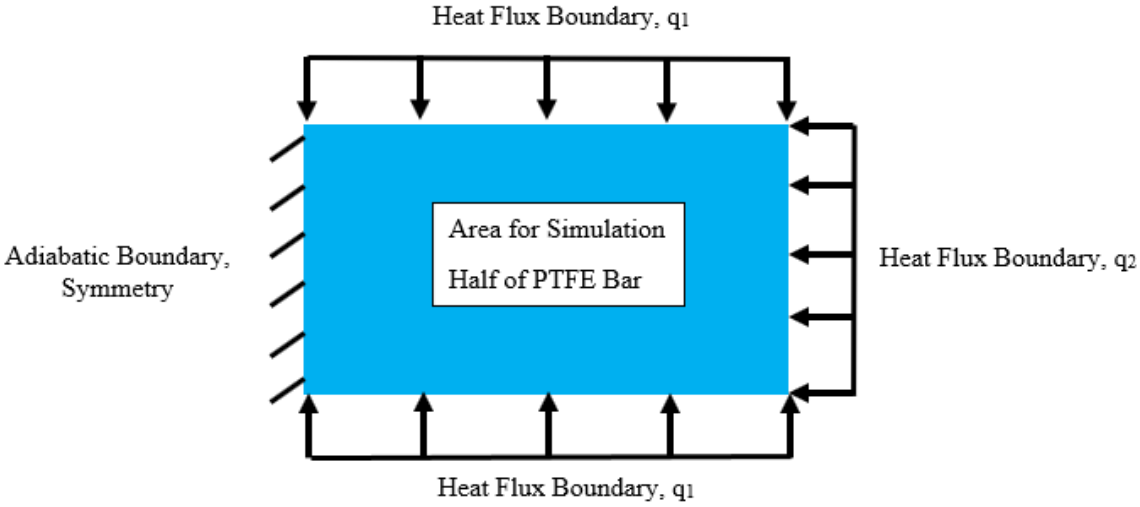

Figure 19: Boundary conditions for the 2-D simulation area used in the MATLAB model

Because the simulation area was only half of the face of PTFE, the left face was modeled as an adiabatic boundary due to symmetry. The top and bottom faces were both modeled as a heat flux boundary with $q = q_1$. The right face boundary was set to $q = q_2$. The top and bottom faces were modeled with the same heat flux because they both contain two cartridge heaters. The right face was modeled with a separate heat flux because the sides do not have heaters in them. Thus, the sides heat up due to the conduction throughout the heater dies, but they do not contain heater cartridges directly in the sides.

The values for the heat flux boundaries were based on the maximum heater power and tuned to reflect the current process. The cartridge heaters have a maximum rated power output of 600 W. Thus, the heat flux on the material at any given time could not be greater than this maximum power. As mentioned before, the controllers give a power percentage displayed throughout the welding cycle. The percentage given on the controller was taken to be a percentage of this maximum rated output of 600W. This power percentage was observed throughout the cycle and summarized data is presented in Figure 20.

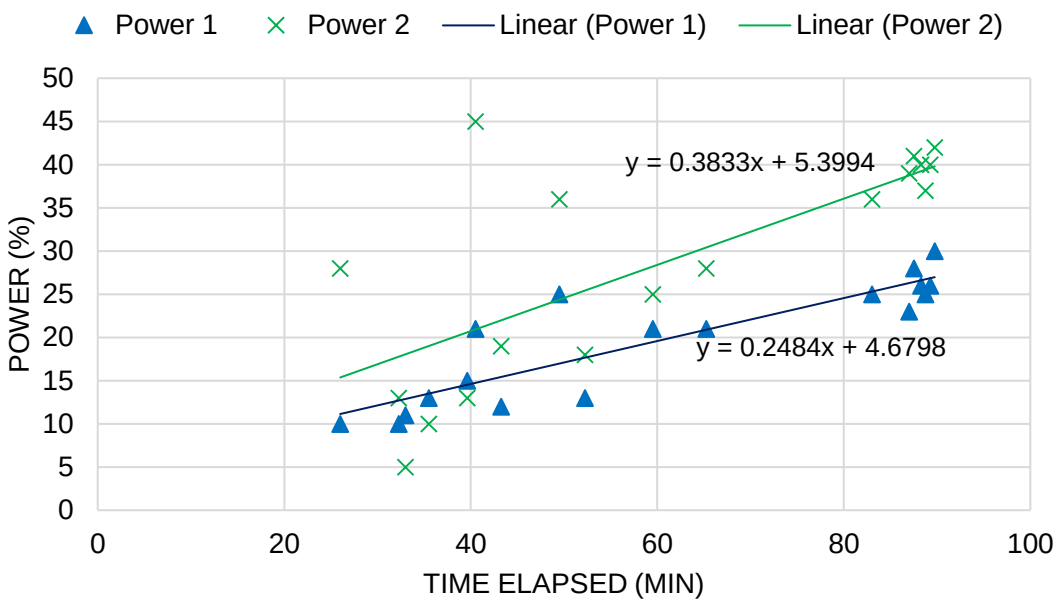

Figure 20: Observed heater power percentage of the top and bottom heaters over the 90-minute weld segment

The heater data is very inconsistent as shown. This is because the controllers turn the heaters on and off based on the thermocouple feedback. If the heater temperature varies greatly from the target program, it will drastically affect the percentage of power. Though the data is somewhat unclear, the power shows a linearly increasing slope from about 5-10% to approximately 25-40%. For the MATLAB model, the heat flux for the boundaries was a linearly increasing slope to a maximum value where it then became constant after a specified time. During the linearly increasing portion, the power percentage increased from 5% to 25%. The heat flux was calculated from power and area, $Q_{max} = 600W$ and $A = 0.160\, m^2$. The area used for this calculation was taken to be the area of the assembly of the heater dies. The initial heat flux was calculated with a constant that could be calibrated. For the calculations, $c_1 = 0.0425$. The value of this constant was calibrated based on validation data. Equation 5 shows the calculation of the initial heat flux.

$$Initial \quad q_1 = c_1 q \tag{5}$$

The equation for the transient heat flux on the top and bottom boundaries was modeled as a simple linearly increasing value. The equation used in MATLAB is shown below in Equation 6. This equation also had a constant that was calibrated based on validation data. For the predicted data, $c_2 = 0.21$. The heat flux on the right side of the material was taken to be 20% of the heat flux on the top and bottom as shown in Equation 7.

$$q_1 = q_1 + c_2 dt \tag{6}$$
$$q_2 = 0.2 q_1 \tag{7}$$

These equations were used to model a linearly increasing slope for the heat flux for the first 60 minutes of the 90-minute cycle. After 60 minutes, the heat flux remains constant. The heat flux values had to be assumed and were later verified as discussed in the Verification & Validation section.

3.4.2 Nodal Equations

The finite difference method was used to calculate the 2-D temperature distribution. The top, bottom, and right side used the equation for a heat flux boundary from *Heat Transfer* (Mills, 1992). The equations for the corner nodes were derived using the energy balance method for the 2-D transient finite difference method. The derivations of the corner nodal equations are shown

below for the finite difference method. Figure 21 below shows the reference for the corner node locations.

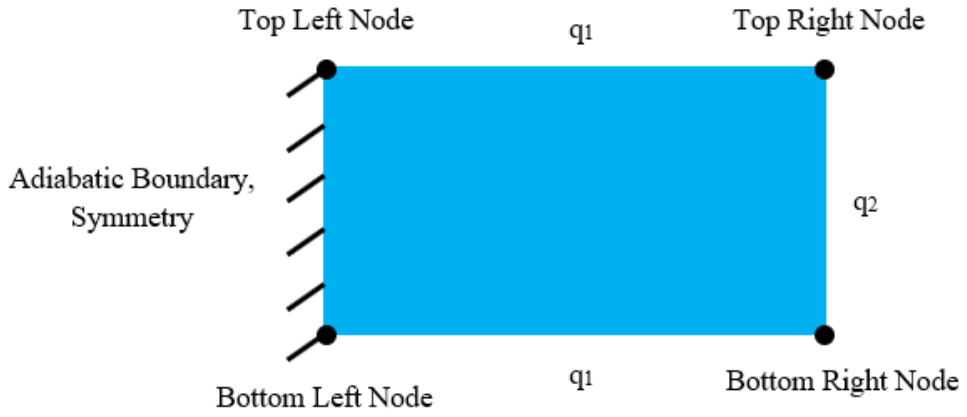

Figure 21: Boundaries and corner nodes for MATLAB model area of simulation

Figure 21 shows the boundaries on the PTFE area used in the simulation. The right face had a heat flux boundary, q_2. The top and bottom boundaries had a heat flux, q_1. The equations for the corner node boundaries were derived using an energy balance method as outlined by Mills (Mills, 1992). Figure 22 shows the boundaries for the top left node.

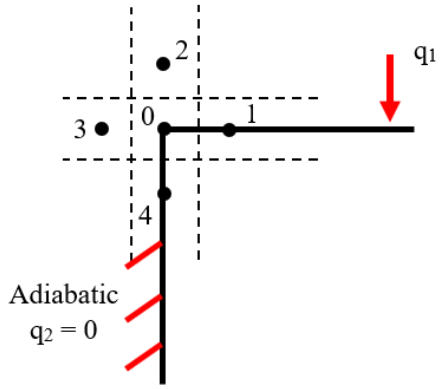

Figure 22: Finite difference equation derivation for the top left corner node of the weld face

Application of the energy balance method and substitution for the top left corner node yields

$$T_0' = \frac{1}{2}F_0\left[(T_1 + T_4) + \frac{\Delta x}{k}q_1\right] + T_0(1 - F_0) \qquad (8)$$

Where to be valid, $\Delta x = \Delta y$. For stability of this equation, $F_0 < 1$. Similarly, the bottom left corner node had a face with a heat flux and an adiabatic face as shown in Figure 23.

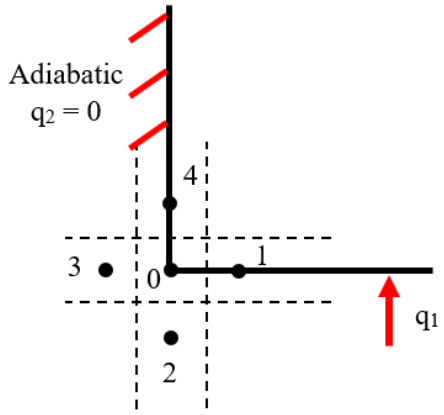

Figure 23: Finite difference equation derivation: bottom left corner node of the weld face

Because this corner had the same boundaries as the top left node, Equation 8 could be used also for this nodal equation. Next, the top right corner nodal equation was derived. The boundaries for the top right corner node are shown in Figure 24.

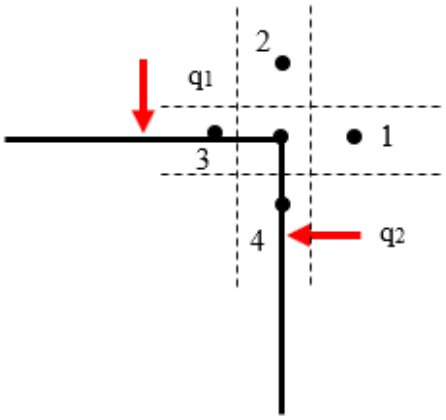

Figure 24: Finite difference equation derivation: top right corner node of the weld face

As shown, there were heat fluxes on both the top and right faces, q_1 and q_2. Application of the energy balance method and substitution for the top right corner node yields

$$T_0' = F_0\left[\frac{1}{2}(T_3 + T_4) + \frac{\Delta x}{2k}q_1 + \frac{\Delta x}{2k}q_2\right] + T_0(1 - F_0) \qquad (9)$$

where $\Delta x = \Delta y$ for validity and $F_0 < 1$ for stability. This equation is similar to Equation 8 with the exception that there is an additional heat flux term. The bottom right corner node also had the heat fluxes, q_1 and q_2 on its boundary faces. The diagram for the boundaries is shown in Figure 25.

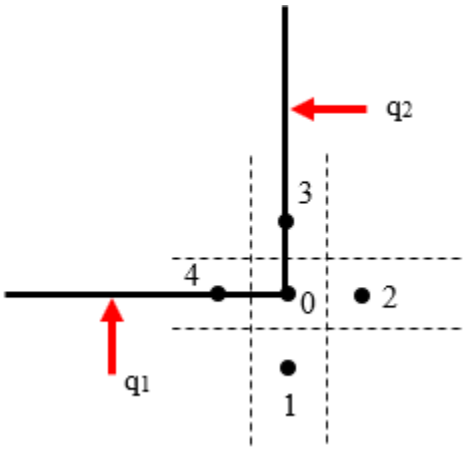

Figure 25: Finite difference equation derivation: bottom right corner node of the weld face

Because the boundaries were the same for the bottom right corner and the top right corner, the same equation was used for both. The only difference between the two are the location of the nodes, but the finite difference equation was the same. For the nodes along faces with heat flux boundaries except for the corners, Equation 10 was used from *Heat Transfer* (Mills, 1992).

$$T_0^{i+1} = 2F_o\left[T_0^i + \frac{1}{2}\left(T_i^2 + T_3^i\right) + \frac{q_s^i \Delta x}{k}\right] + (1 - 4F_o) + T_0^i \qquad (10)$$

For this equation to be valid, $\Delta x = \Delta y$ and $F_0 < \frac{1}{4}$ for stability. This equation was used for all the boundary faces except the corner nodes. On the adiabatic face, $q_s^i = 0$. For the interior nodes, Equation 11 was used from *Heat Transfer* (Mills, 1992).

$$T_0^{i+1} = F_0\left(T_1^i + T_2^i + T_3^i + T_4^i\right) + (1 - 4F_0)T_0^i \qquad (11)$$

Again, for validity and stability, $\Delta x = \Delta y$ and $F_0 < \frac{1}{4}$. There was a total of nine nodal equations used in the numerical solution: four boundary corners, four boundary faces, and one equation for the interior nodes.

3.5 Initial Conditions

The initial condition of the PTFE material being welded was that it was at ambient temperature throughout at the start of the welding cycle. At time t = 0, the temperature of the PTFE bar is equal to the ambient temperature. For the MATLAB model, ambient temperature was taken to be $T_0 = 23°C$. This temperature was set at each node throughout the PTFE simulation area using for loops for nodes in both the M and N directions.

3.6 Numerical Solution: Nodal Mesh Size

The solution for the temperature distribution in the PTFE area simulation was based on the finite difference method for 2-D transient heat conduction. To ensure accurate calculations, there were a few important factors that were kept in mind such as: the number of nodes, the Fourier number, and the material properties. In the MATLAB model, the number of nodes was carefully chosen. M represented the number of nodes in the x direction, where N represented the number of nodes in the y direction. Because of the way MATLAB arranges matrix indices as rows, then columns, the temperature matrices used a format as: T(N, M). Although this seems contradictory to convention, this ensured that the displayed temperature matrix displayed the values in the directions as shown in Figure 26.

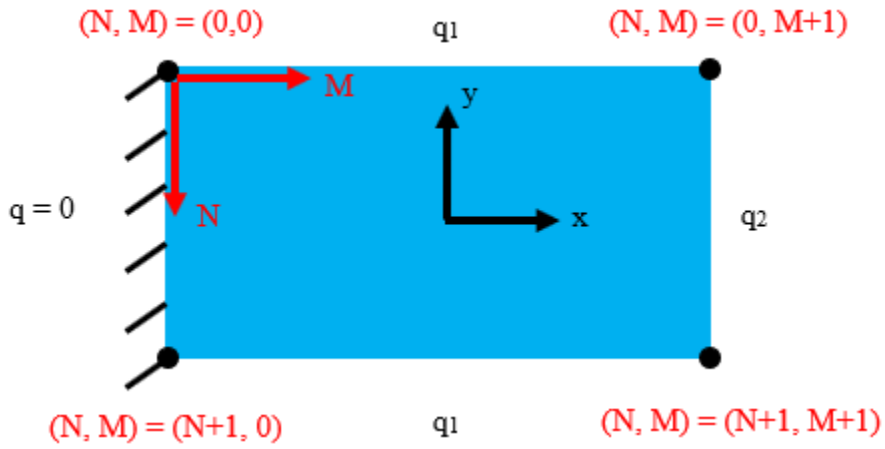

Figure 26: Corner nodes of the PTFE area simulation for the MATLAB model

As displayed, the top left corner node had indices of (0, 0) with nodal coordinates increasing down and to the right in the N and M directions. The total number of nodes in the x

direction was M+1, and the total number of nodes in the y direction was N+1. The distance between each node in the x direction was dx and the distance between each node in the y direction was dy. For the validity of the nodal equations, dx = dy. The nodal equations for the heat flux boundaries and the interior nodes were taken from *Heat Transfer* while the equations for the corner nodes were derived. Based on the dimensions of the PTFE bar, the number of nodes in the N direction was chosen, then dx and the number of nodes in the M direction were calculated. The number of nodes was chosen for the N direction rather than the M direction because the height is a smaller dimension. The number of nodes chosen for the height was N+1 = 38 as this gave the least amount of error in the length in the M direction. The calculations for this number of nodes are shown in the Appendix, Table 9. Once the number of nodes in the N direction was chosen, dy was calculated as below.

$$dy = H/N \tag{12}$$

For validity of the finite difference equations

$$dx = dy \tag{13}$$

Then, M the number of nodes in the x direction was rounded from the length divided by the mesh distance

$$M = round\left(\frac{L}{dx}\right) \tag{14}$$

M needed to be an integer so that the code worked properly because it was used as the number of times a for loop was calculated. To ensure it was an integer, the round function was used. This means that the length L in the model would be off by an amount of dx. However, with a small enough dx, the error in this length would be minimal. As shown in Table 9, the error in L was minimized to 3.55×10^{-16} in and thus can be taken as zero. The number of nodes used for the calculations was N+1 = 38 and M+1 = 78 to ensure that the error in the length was minimized. Based on the way the code works, the total number of nodes is one value greater than the values used in N and M, or N+1, M+1. If this distance was not minimized, it could cause errors in the calculations, but this small of an error does not affect the calculations.

Also important for the accuracy of the calculations was the chosen time step for the transient response of the heat conduction. For this model, a time step of $\Delta t = 0.1$s was chosen. A time step of 1s was first tried; however, the Fourier Number became unstable and thus the time step was reduced. More time could have been spent determining at what value the simulation becomes

unstable to reduce the calculation time, but the time step of 0.1s provided stable results which will be discussed further in the Verification & Validation section.

3.7 Results

3.7.1 Current Design

The following results are outputs from the MATLAB model. These results represent the characteristics of the current welder design using Segment 1 of Program 1. During segment 1, the controller prescribes a ramp time from 60°F to 700°F. This program shows what is believed to be an accurate representation of the current process. The following results are the calculations from the model under the conditions that have been discussed with the material starting from ambient temperature. The model calculates and displays information about the temperature distribution, transient response, material properties, and the power input into the material. The first set of results is representative of the total cycle time of the first 90-minute segment. Later, the temperature distribution for the first 15-minutes will be shown. The first output shown below in Figure 27 is a plot that shows the temperature distribution in the adiabatic face in the center of the material every 15 minutes.

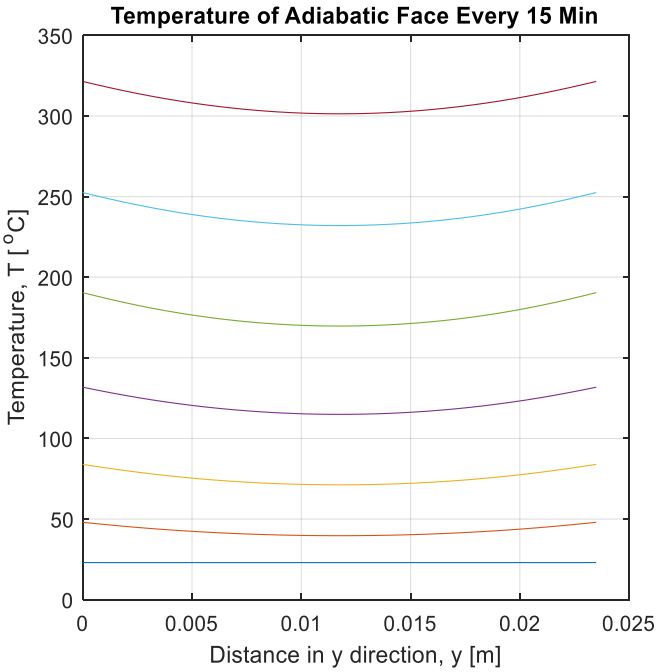

Figure 27: Transient temperature response of the adiabatic face of the PTFE at 15-min intervals

The adiabatic face was of interest because this is generally where the weld fails if the weld does not go all the way through the material. In the plot, the curves progress up with time. The bottom flat line is the initial temperature distribution in the material and the top curve is after 90-minutes. As shown, the adiabatic face was initially at the ambient temperature. Then, with each progressive temperature curve, the material increases temperature, but the top and bottom faces increase more. This can be seen at the ends of each curve. The ends of the curve start to bend upwards more with each progression, indicating that the temperature difference increases throughout the cycle. The next output from the model was the temperature distribution in the face of the PTFE bar in Figure 28.

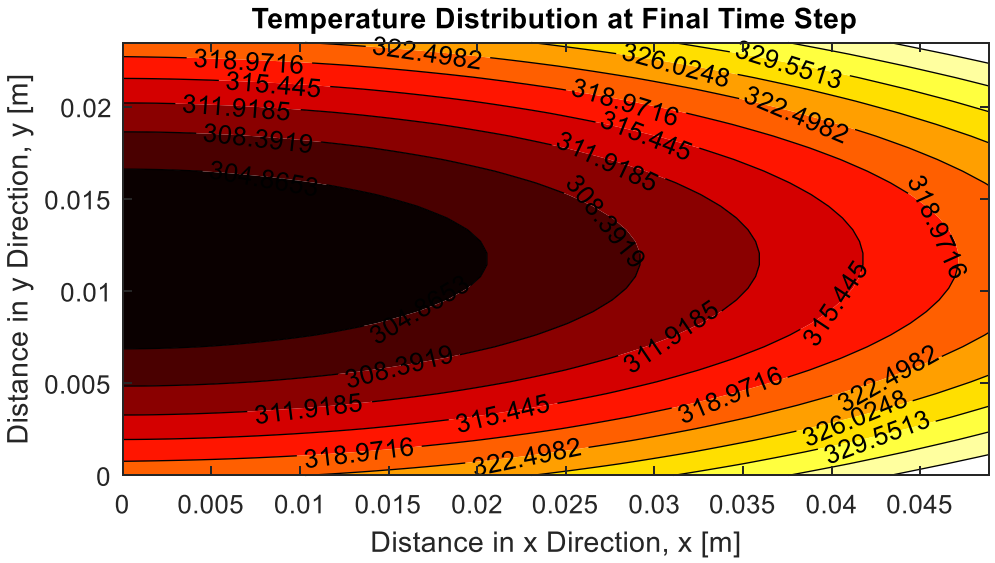

Figure 28: Temperature of the PTFE from the MATLAB model after the 90-min weld cycle

The temperature distribution shown was the main focus from the model. As will be later discussed, this output was compared to a similar distribution that was taken from a thermal camera of the material. The important characteristics from this plot were the temperatures of the top and center on the adiabatic edge, and the temperature difference between the two. This will be discussed further in the Verification & Validation section. The next plot outputs were the transient heat flux loading on the material in Figure 29 and the transient temperature response of the top left node in Figure 30.

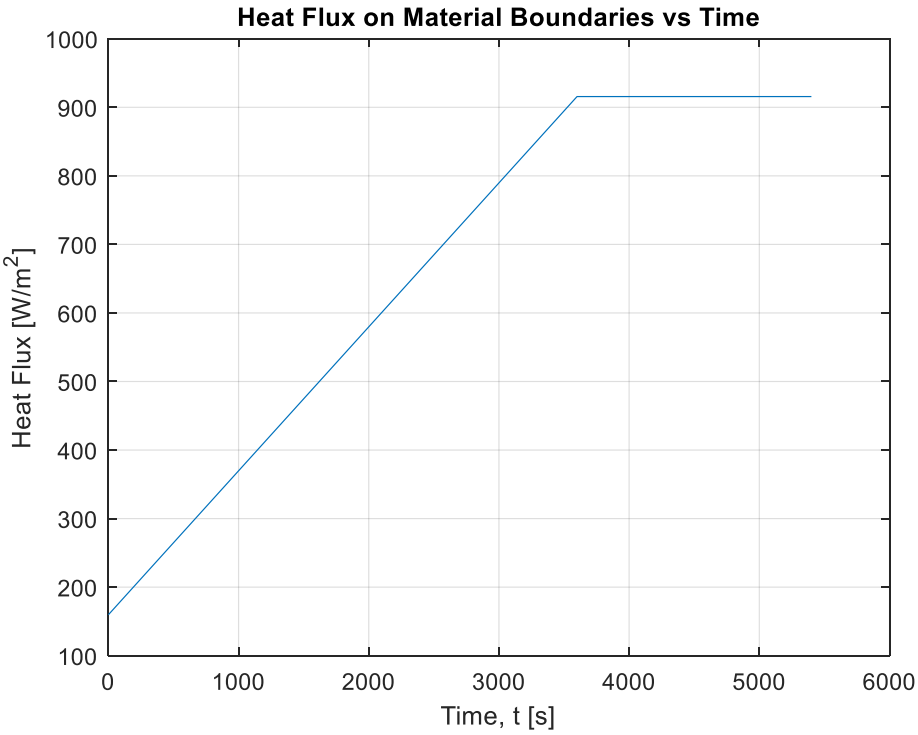

Figure 29: Transient heat flux loading on the PTFE for the 90-min weld segment

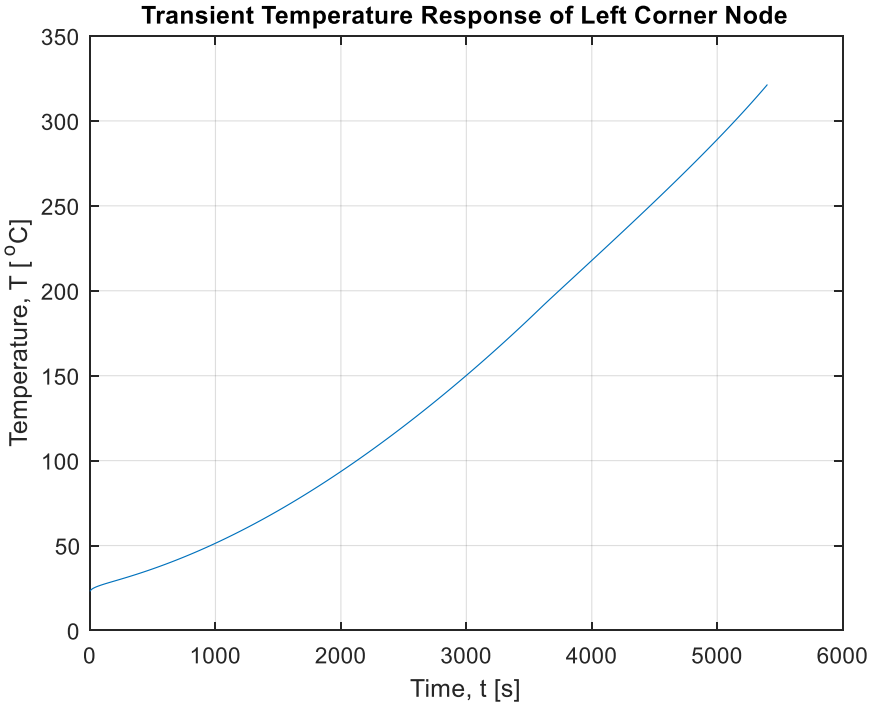

Figure 30: Transient temperature response for the top left corner node through the 90-min weld segment

The transient heat flux is represented in Figure 29. This is the heat flux loading that is on the material itself and not the input into the dies. The curve shown is the heat flux input into the top and bottom faces of the material. The input onto the right face was 20% of the amount on the top and bottom faces. As shown in the plot, the heat flux linearly increases with time for 1 hour and then is constant for the remaining half hour of segment 1. Also calculated were the maximum and minimum power which were about 150W and 25W respectively. The maximum power on the material was about 25% of the total heater power. This coincides with the observed maximum power of 25-40% from the heater controller.

In Figure 30, the transient response of the top left node is shown. This curve had a relationship with the heat flux input on the material. As the heat flux was linearly increasing for the first hour, the temperature had a parabolically increasing response. When the heat flux was constant, the temperature correspondingly had a linearly increasing response. The heat flux is close to a derivative of the temperature response. Of additional interest from this model were the material properties as a function of time as well as how the properties varied through the material at the final time step. Plots for each of these were displayed for the thermal conductivity, the specific heat, and the density of PTFE. To save space, the plots for these material properties will be displayed on the next three pages and then discussed on the following page. For thermal conductivity, Figure 31 shows a distribution of how the property varies with temperature in the face of the PTFE material. Figure 32 shows the transient response of the thermal conductivity over time for the top left node. For the specific heat of PTFE, Figure 33 shows a distribution of how the property varies with temperature in the face of the PTFE material at the final time step. Figure 34 shows how the specific heat varies over time for the top left node. Similarly, Figure 35 shows the distribution of the density of the material at the final time step and Figure 36 shows the transient response for the top left node.

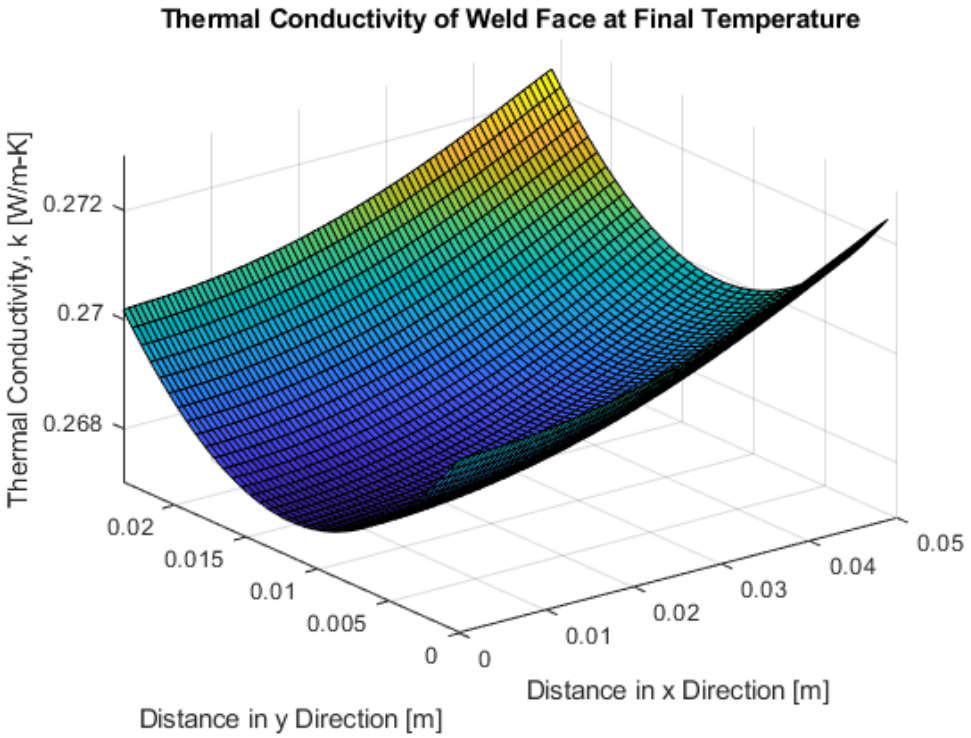

Figure 31: Variance of the thermal conductivity in the PTFE after 90-min

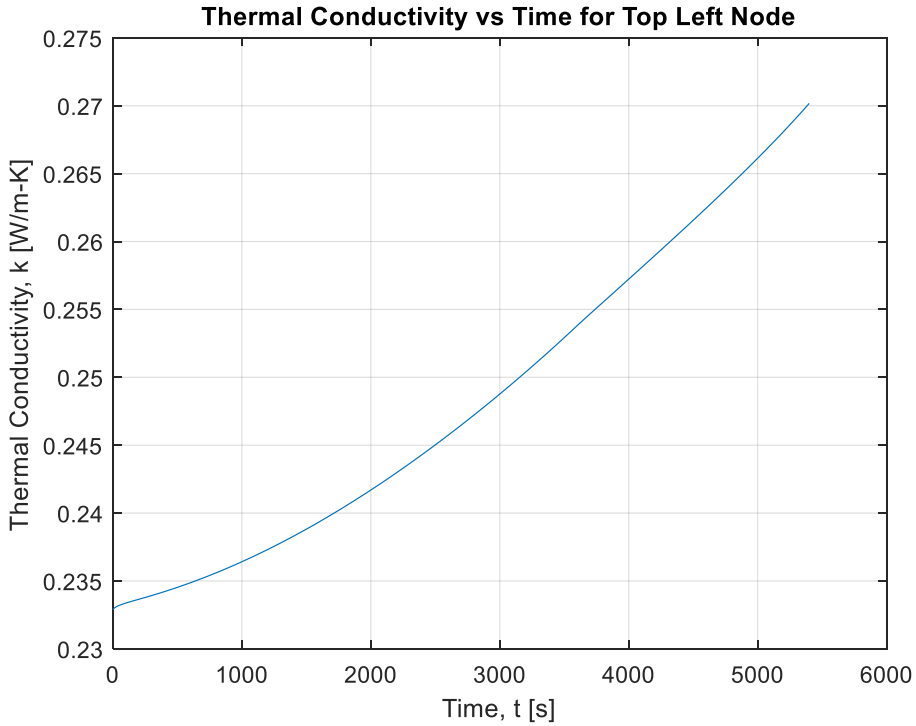

Figure 32: Transient response of thermal conductivity for the top left node over 90-min

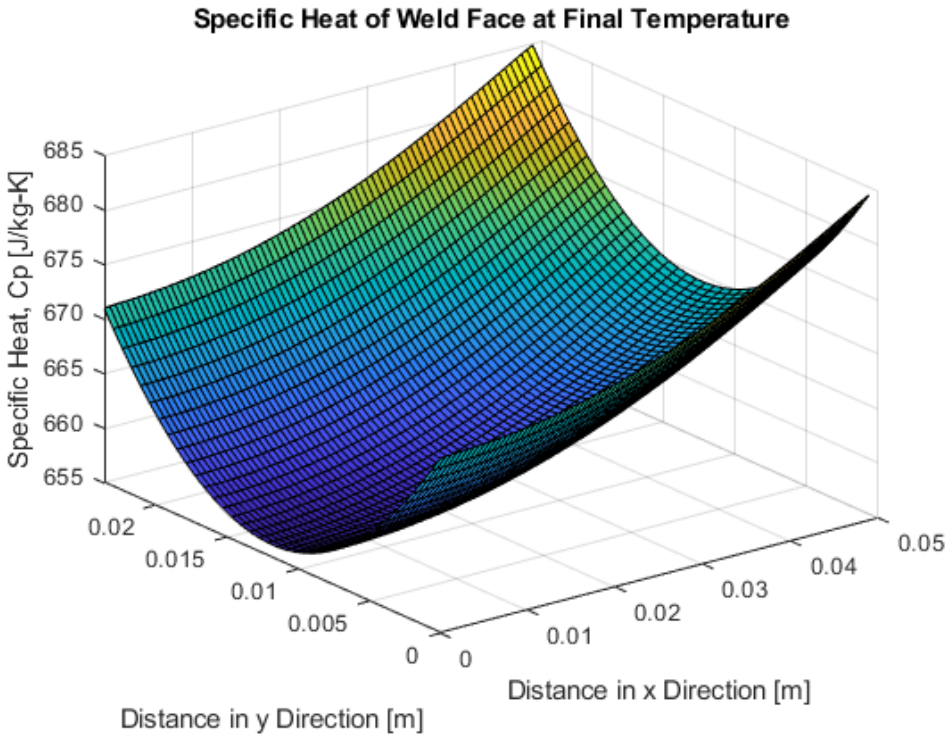

Figure 33: Variance of the specific heat in the face of PTFE after 90-minutes

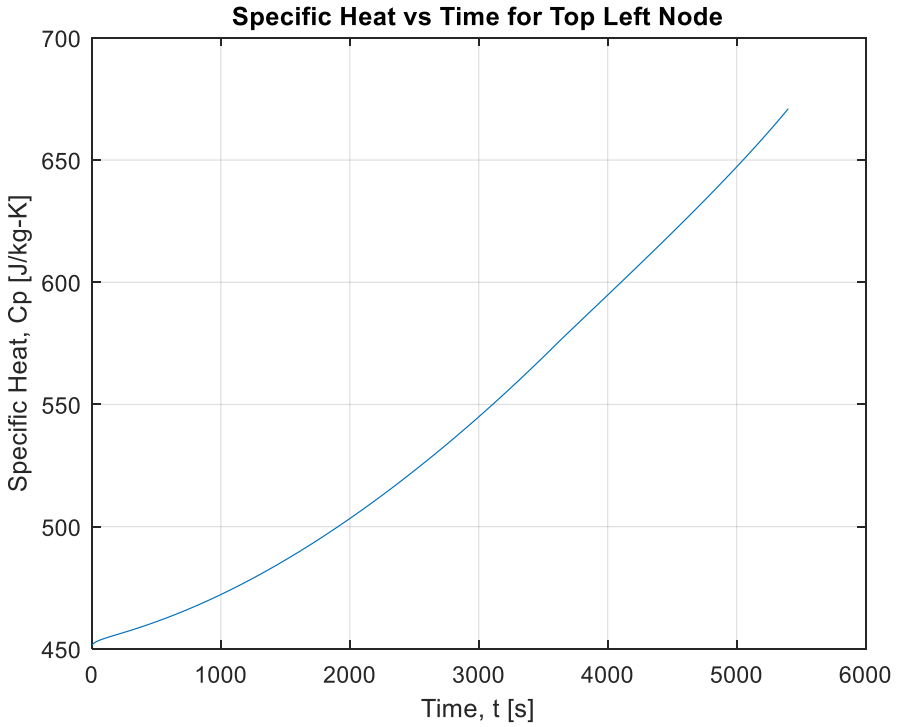

Figure 34: Transient response of the specific heat for the top left node after 90-min

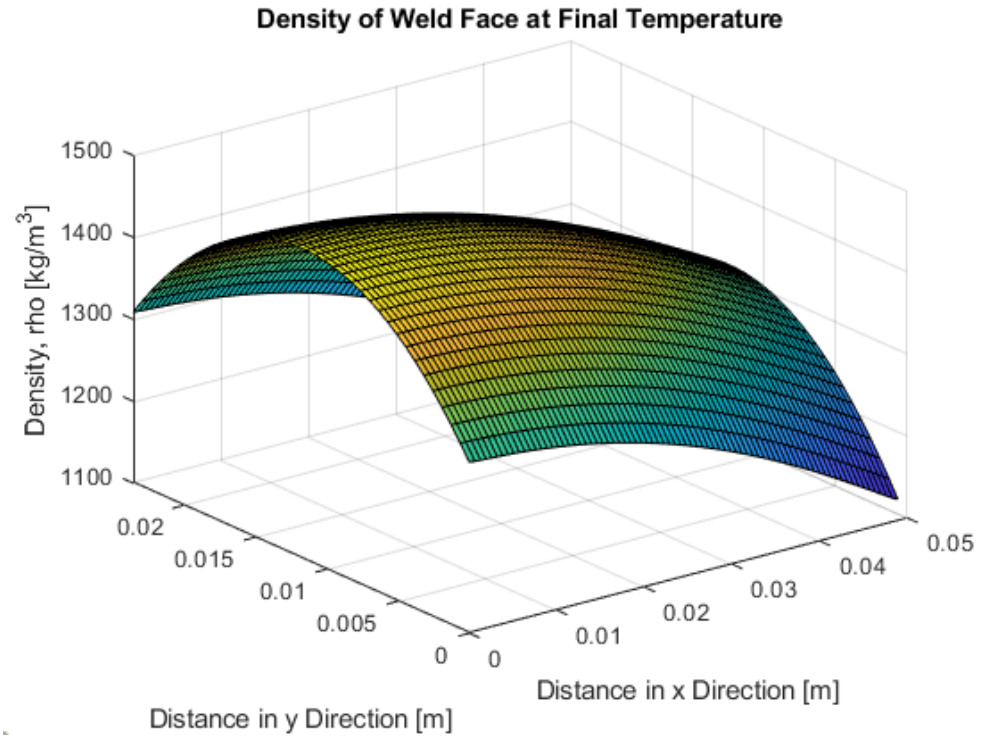

Figure 35: Variance of the density in the face of PTFE after the 90-min weld segment

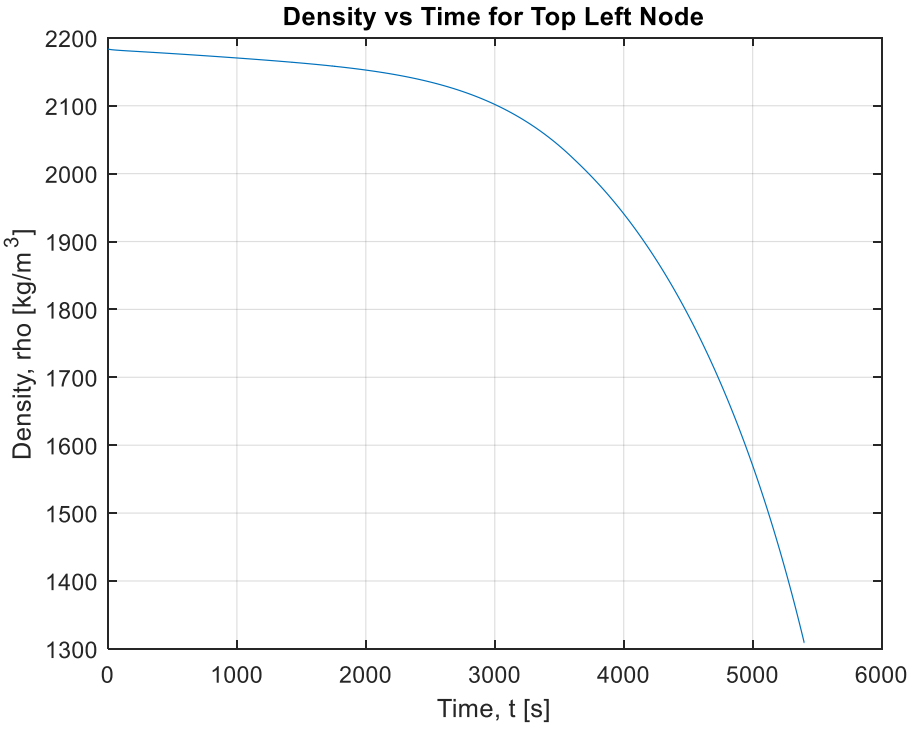

Figure 36: Transient response of the density for the top left node after 90-min

The thermal conductivity of PTFE varies only slightly throughout the material with varying temperature. From the scale of the graph in Figure 31, it can be seen that the thermal conductivity ranges only from 0.26 to 0.275 W/m-K throughout the material at the final time step. The hottest portions of the material reflect the places where the thermal conductivity is the highest. Because the edges are at the highest temperature, the graph shows a parabolic shape with the edges having the highest thermal conductivity. The surface plot of the specific heat shows similar contours with the edges having the highest values. The specific heat however varies more throughout the face of the material. The transient response for the thermal conductivity and specific heat show similar parabolic curves with the specific heat varying more. These properties show similar curves as they both increase linearly with increasing temperature. The density however varies differently than these two properties. The density decreases with a parabolic curve as a function of temperature.

Other characteristics of interest were the temperature differences of the right and left faces of the material and the maximum and minimum heater power on the material throughout the simulation. Below are some of the characteristics calculated from the model:

```
Delta T of Adiabatic Face [C] =
   20.0525
Delta T of Right Face [C]=
   19.9804
Maximum Power Input [W]: Qmax =
  146.2101
Minimum Power Input [W]: Qmin =
   25.5034
```

The temperature difference of the adiabatic face was used for validation and will be discussed further in the Verification & Validation section. It was important to verify the model at more than a single time interval which will also be discussed in the Verification and Validation section. For validation, the model was calculated at time intervals of 90-minutes and 15 minutes.

Next, the results from the 15-minute time interval will be shown. Figure 37 shows the temperature vs distance in y along the adiabatic face for every 2.5 min interval. The bottom line shows that the material starts out at ambient temperature throughout. Then each line up is a consecutive 2.5-minute interval. The temperature difference along the face increases with each interval, indicated by the increasing upwards slope of the temperature curves.

The final temperature distribution in the weld face after 15 min is displayed in Figure 38. As seen, the temperature difference is less than after 90 min as expected. This plot will be further used for the verification of the model. The next figures will be discussed on page 65.

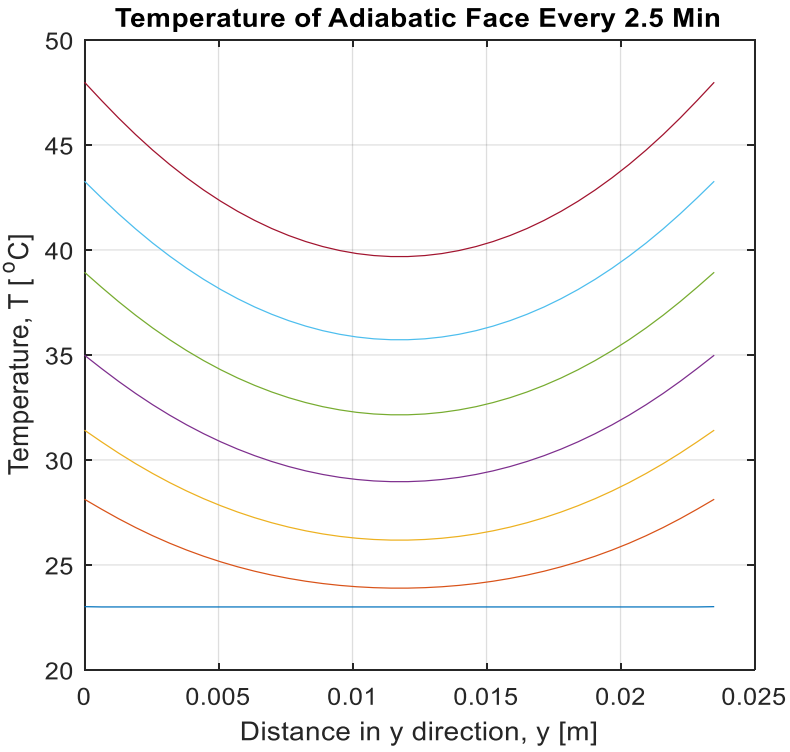

Figure 37: Transient temperature response of the adiabatic face of the PTFE at 2.5-min intervals

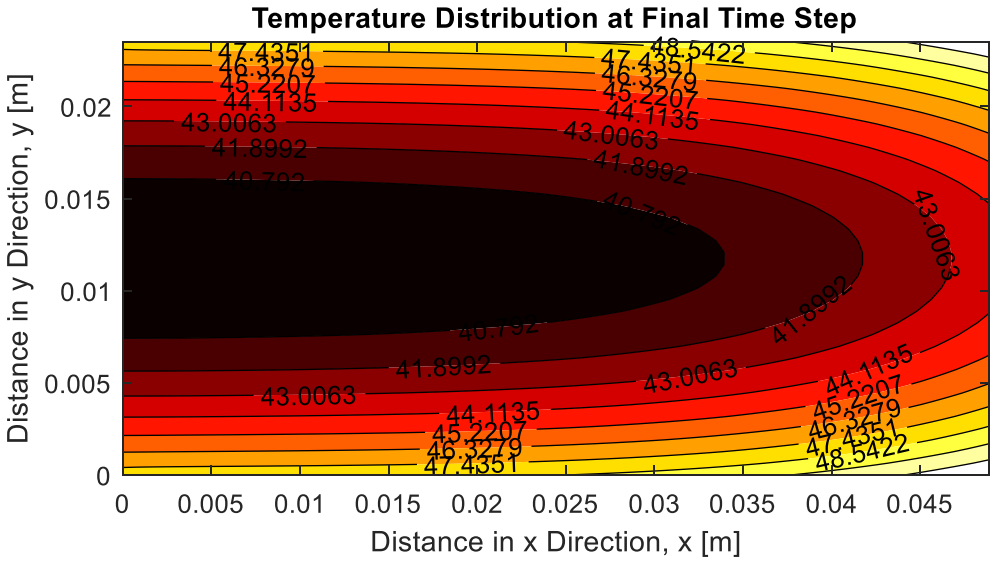

Figure 38: Temperature of the PTFE from the MATLAB model after 15-min

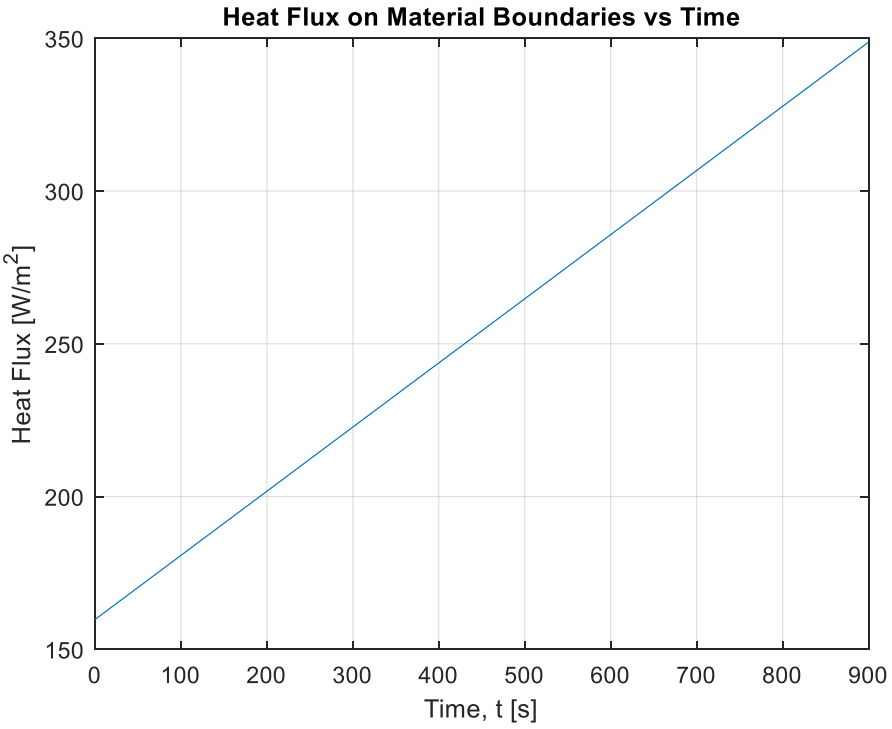

Figure 39: Transient heat flux on the top and bottom boundaries: 15 min interval

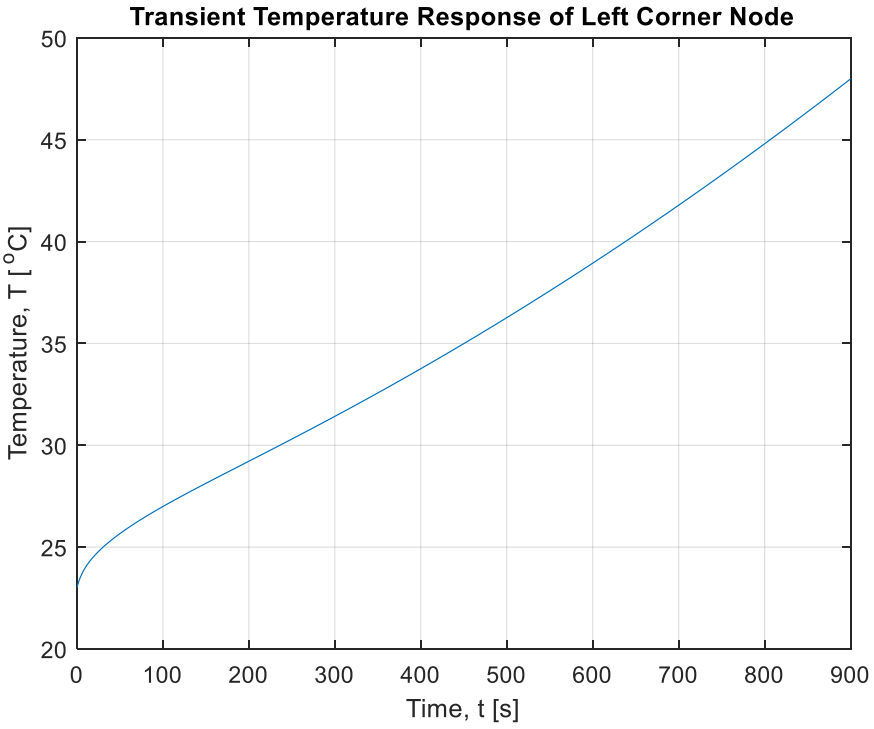

Figure 40: Transient temperature response of the top left corner node: 15 min

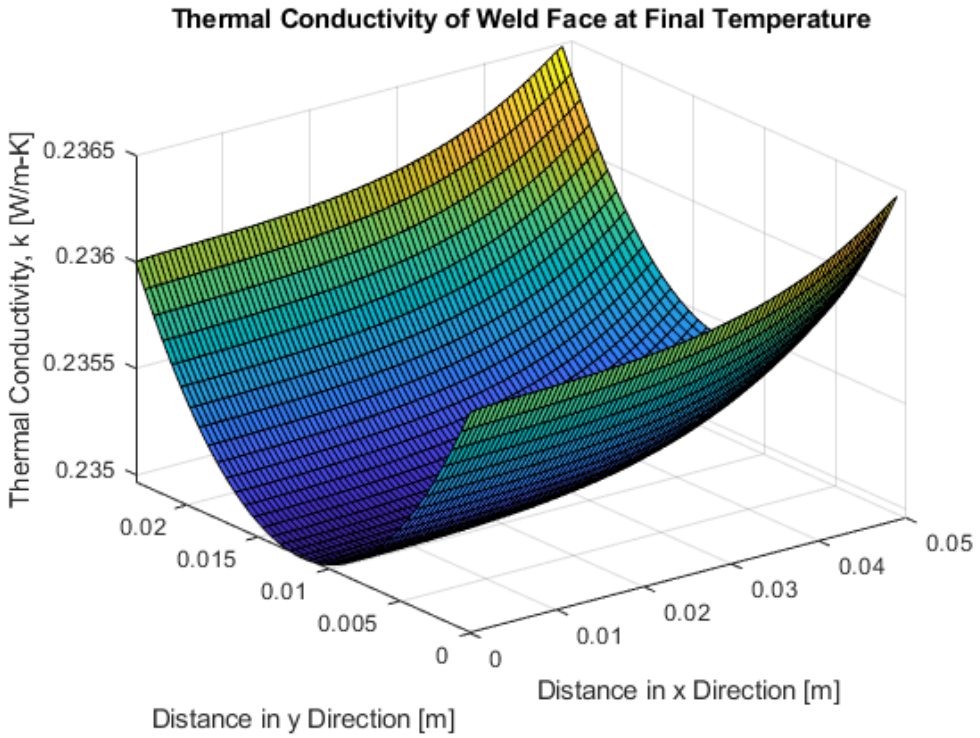

Figure 41 Variance in the thermal conductivity of the face of PTFE after 15 min

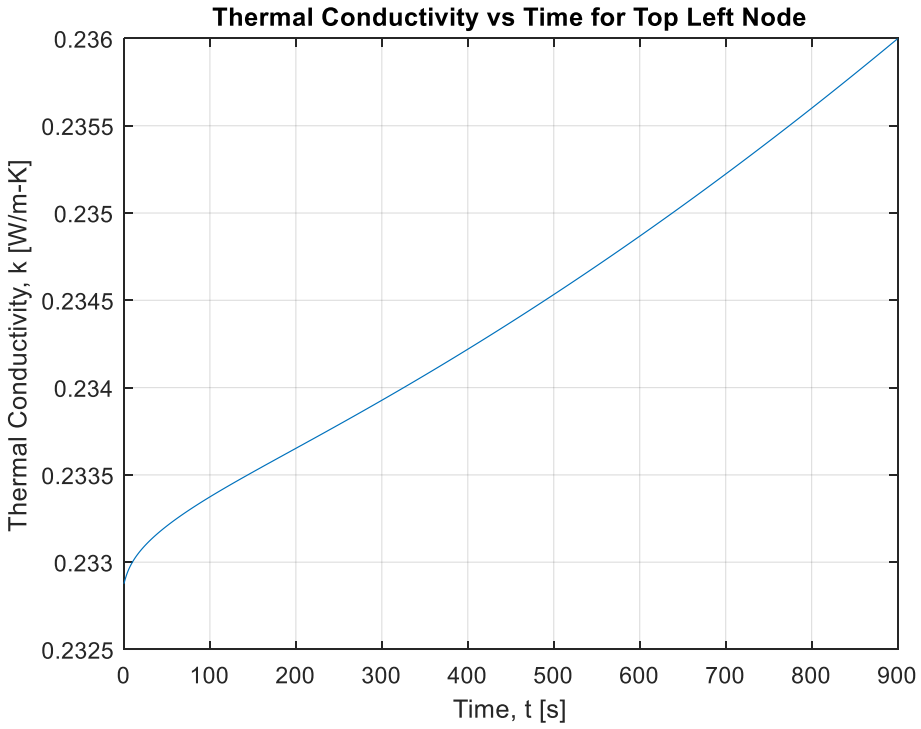

Figure 42: Transient thermal conductivity response of the top left node through 15 minutes

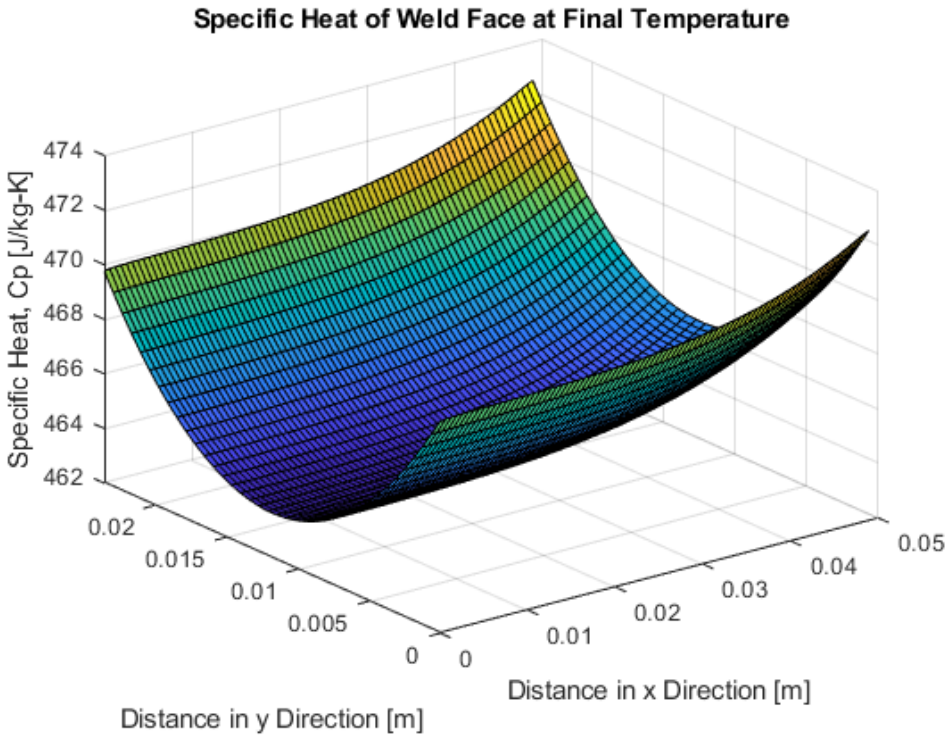

Figure 43: Variance in the specific heat of the face of PTFE after 15 min

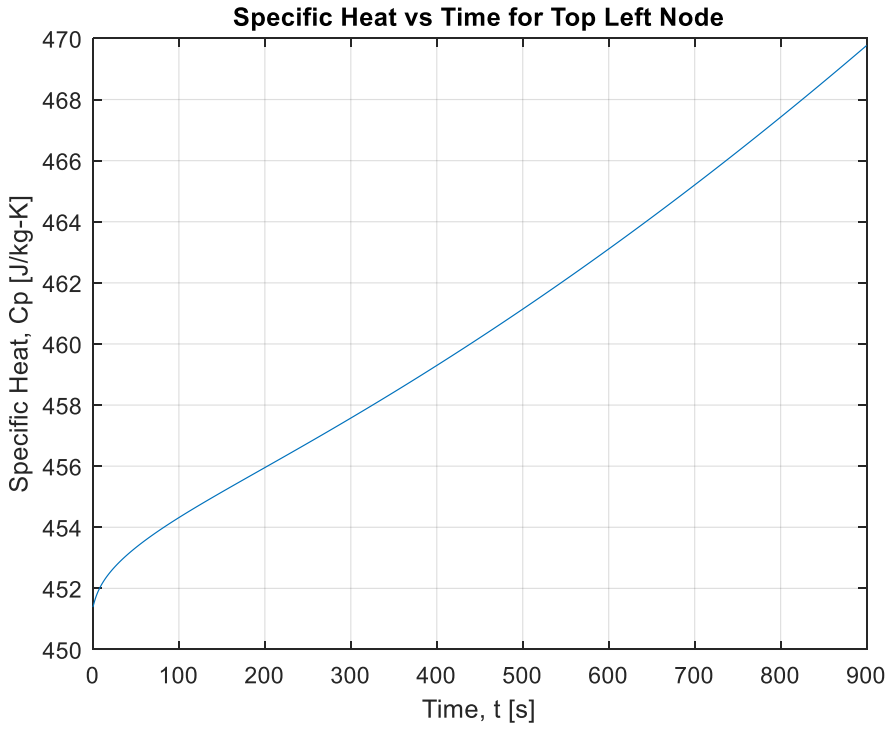

Figure 44: Transient response of the specific heat of PTFE of the top left node: 15 min interval

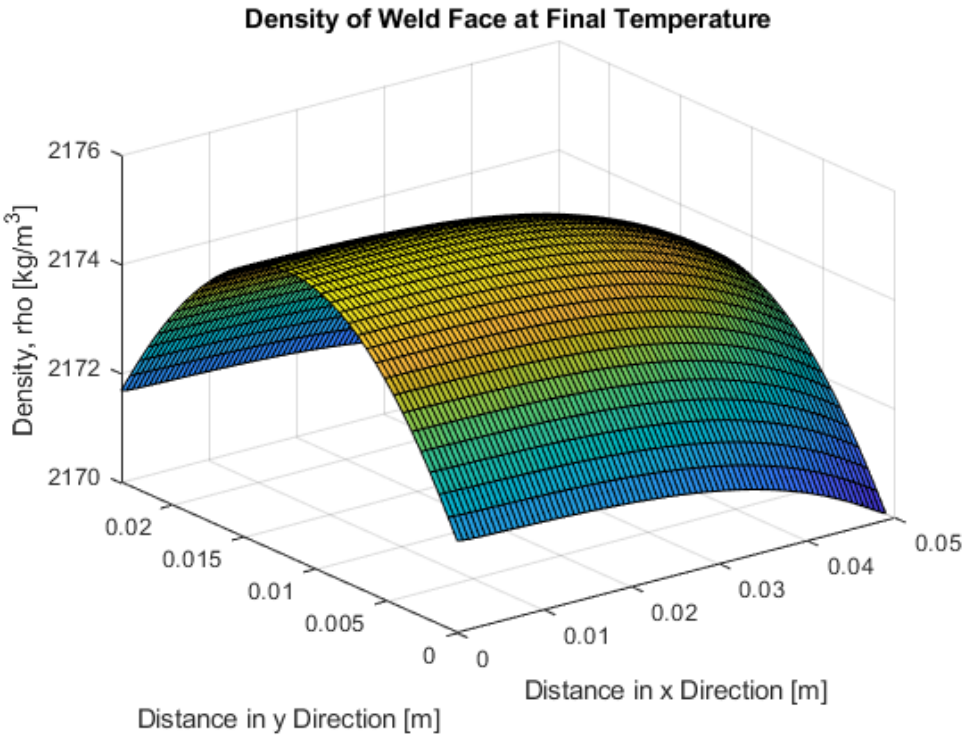

Figure 45: Variance in the density of the face of PTFE after 15 min

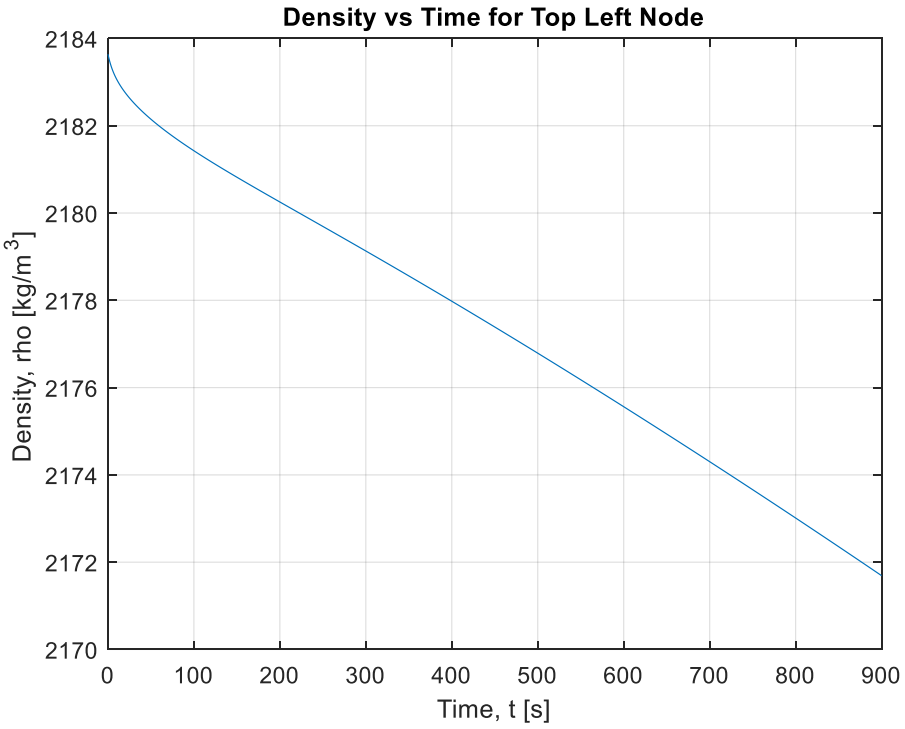

Figure 46: Transient density response of PTFE of the top left node for 15 min interval

Figure 39 shows the transient heat flux on the top and bottom boundaries during the 15-minute interval. During this interval, the heat flux is linearly increasing and does not become constant. As shown the heat flux increases from about 160 W/m^2 to about 350 W/m^2, or about 10% of the heater power. Figure 40 shows the temperature response of the top left node during the 15-minute interval. Because the heat flux is a linearly increasing value, the temperature responds in a gradual parabolic curve. Figure 41 through Figure 46 show the behavior of the material properties through the transient heating cycle. Figure 41 shows the thermal conductivity in the PTFE face after 15 minutes. This shows that at the edges of the material, the thermal conductivity is increased; however, the material is all at approximately 0.23 W/m-K. Figure 42 shows the transient response of the thermal conductivity for the top left node of the material. Similar to the temperature response plot, the thermal conductivity increases with increasing temperature. The plots of the specific heat are shown in Figure 43 and Figure 44. These plots show similar results to the thermal conductivity plots because the specific heat also linearly increases with increasing temperature. The specific heat in the material varies from 462 to 474 J/kg-K after 15-minutes. The specific heat of the top left node varies from 452 to 470 J/kg-K over the 15-minute cycle. Lastly, the plots for the density are shown in Figure 45 and Figure 46. Unlike the thermal conductivity and specific heat, the density decreases with increasing temperature. After 15-minutes, the density throughout the weld face only varied 6 kg/m^3 and the density of the top left node decreased only 12 kg/m^3 over the 15-minute cycle. Other outputs from the model calculation are displayed below:

```
Delta T of Adiabatic Face [C] =
    8.3000
Delta T of Right Face [C]=
    8.2677
Maximum Power Input [W]: Qmax =
   55.6784
Minimum Power Input [W]: Qmin =
   25.5034
```

The temperature difference of the adiabatic face and the temperature distribution plot were further analyzed for verification and will be further discussed in the next section. These were the results that were calculated for the current process. The accuracy of these results will be discussed in the Verification and Validation section for both time intervals.

3.7.2 Increased Power

One of the main goals for this project was to see if the process cycle time could be reduced. One design change considered was to increase the maximum power of the cartridge heaters that are used in the heater dies. To simulate this, the MATLAB model was calculated for an increased maximum power of 700W, 800W, and 900W of power for a 90-minute cycle. The temperature distribution results of these simulations are shown in Figure 47, Figure 48, and Figure 49 respectively.

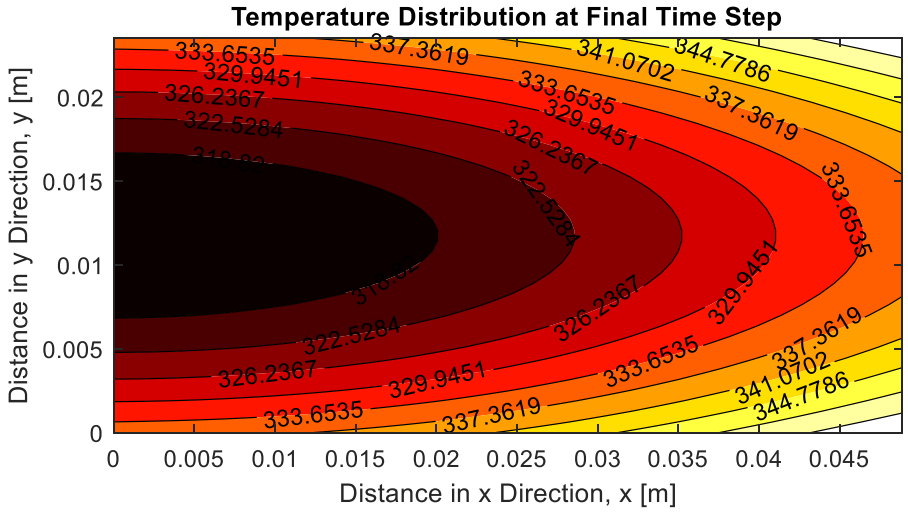

Figure 47: Temperature distribution: 90-minutes with increased power: 700w

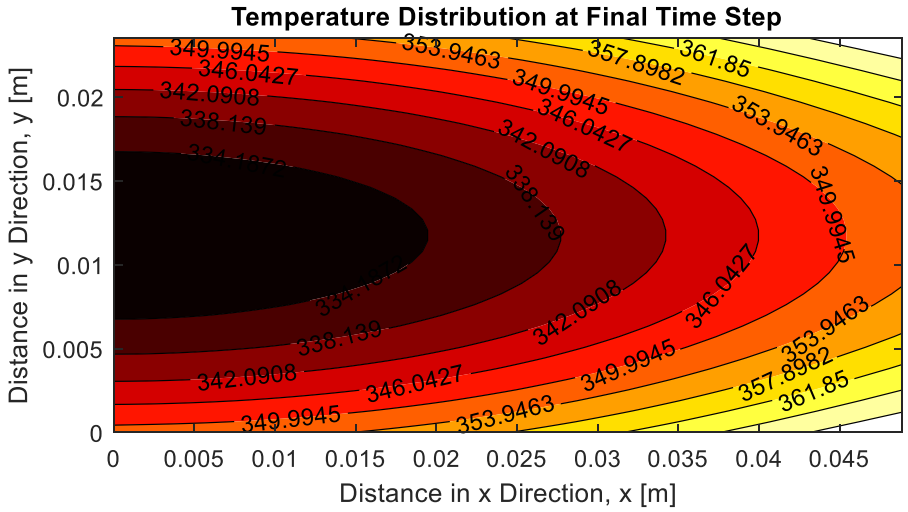

Figure 48: Temperature distribution: 90-minutes with increased power: 800w

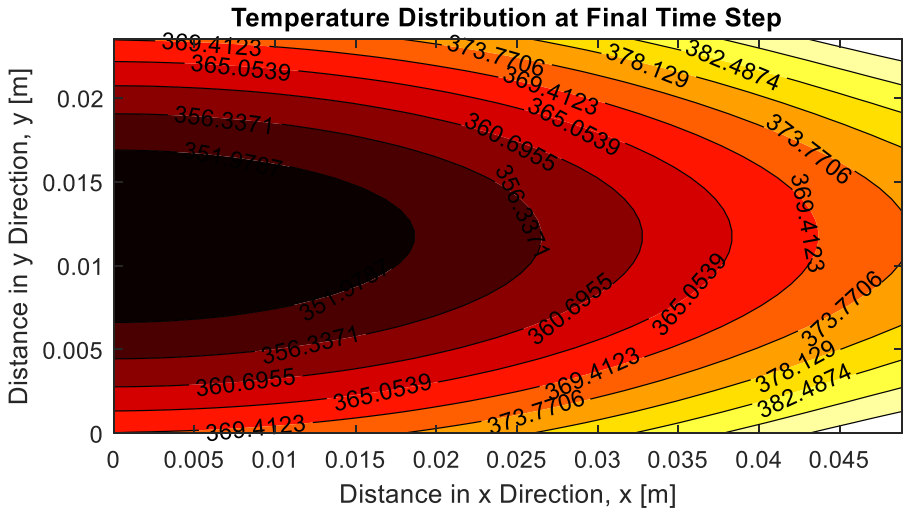

Figure 49: Temperature distribution: 90-minutes with increased power: 900w

With increased power, the overall temperature of the material obviously increases. However, the temperature difference from the boundaries to the center of the material also increases. This could result in a weld that is unsatisfactory. In addition, it is undesirable to have the PTFE material reach a temperature that is above 340°C for sustained periods of time. More investigation would need to be done for validation, but from the preliminary tests, increasing the power would not provide a significant reduction in time as well as a quality weld.

3.7.3 Heated Between the Faces – Semi Infinite Heat Flux Analysis

Another potential design change that was modeled was the semi-infinite heat flux analysis. This analysis represents a hot plate welding method added to the current process. In addition to the current heater die design, this analysis represents the addition of a heater plate in the middle of the two sections of PTFE material to be welded. Figure 50 represents the potential design with the center heater in between the PTFE bar ends.

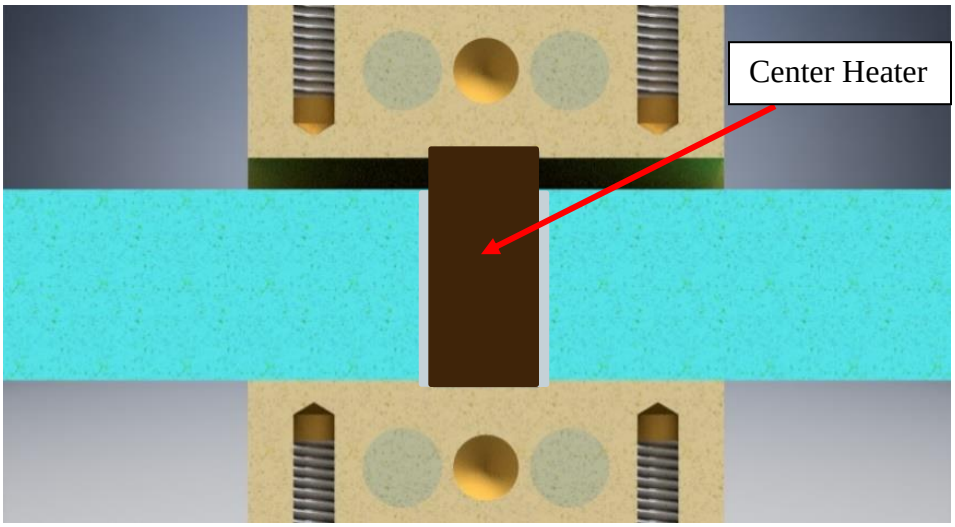

Figure 50: Potential design change with center heater between PTFE pieces

As shown, there would be a heater block in between the faces of the material in addition to the current heater dies for a period of time. The center heater block would then be removed, and the PTFE pieces would be held together under pressure. It was assumed that the center heater block would prescribe a constant heat flux into the face of the material to be welded. It was also assumed that the PTFE was infinitely long in the direction perpendicular to the welded face. These assumptions allowed a semi-infinite heat flux analysis to be calculated for the temperature of the PTFE bar. The equation for the semi-infinite analysis was used from *Heat Transfer* and is shown in Equation 15 (Mills, 1992).

$$T - T_0 = \frac{q_s}{k}\left[\left(\frac{4\alpha t}{\pi}\right)^{\frac{1}{2}} e^{-x^2/4\alpha t} - x\, erfc\frac{x}{(4\alpha t)^{1/2}}\right] \tag{15}$$

The amount of power used for the input into the center heater block was 100W for this analysis. This amount of power was chosen because the current heater dies are thought to input a range of about 25W to 150W into the material during the welding process. For a constant input of 100W into the weld face, the results are shown below in Figure 51.

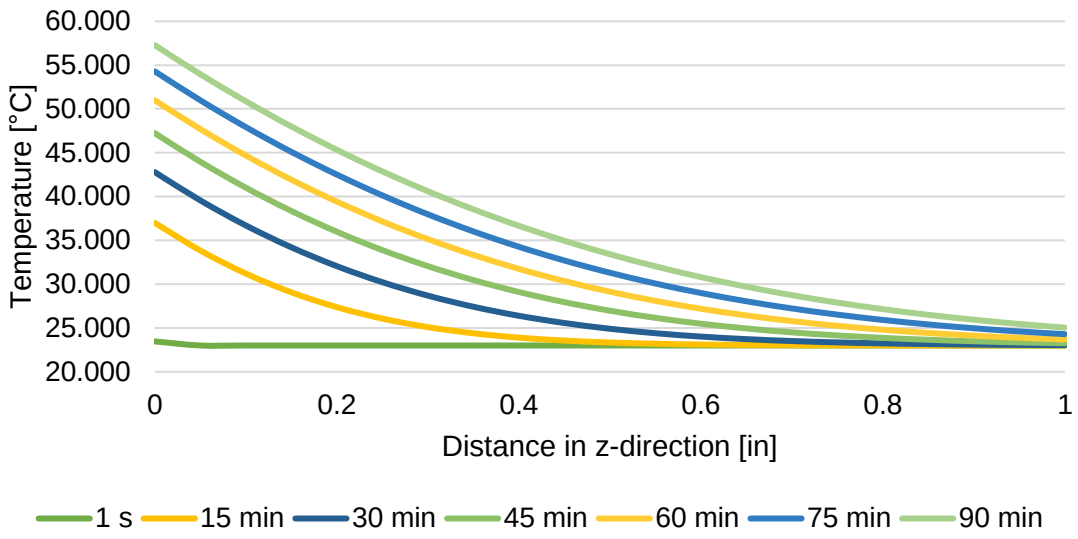

Figure 51: Semi-infinite heat flux analysis on the welded face of PTFE to simulate a hot plate welding method for a 90-min segment of the welding cycle

The plot in Figure 51 shows the temperature of the weld face versus increasing distance in the z-direction, or the direction perpendicular to the weld face at increasing time intervals. The temperature curve was calculated at 15-minute intervals throughout the 90-minute phase used for the previous calculations. These calculations show that with 100W of power in between the two pieces of material, the temperature of the weld face could be raised about 57°C at the weld face, or z=0 at a time of 90-minutes. At a distance of 0.25 in, and at a time of 90-minutes, the temperature of the material could be raised by 43°C. This is significant because approximately 0.25 in of material is the overlap distance of the two PTFE pieces during the welding process.

The MATLAB model was calculated with the additional temperature predicted from the semi-infinite analysis. To simulate the temperature gain of 57°C at the face of the material z=0 after 90-minutes, the model was calculated with this amount added at the final time step. Because the temperature was raised, the total program run time could be reduced. After trials, it was determined that the time could be reduced to 77.5 minutes with this additional heat in between the material. This calculation was for reference because a 2-D analysis is no longer valid when heating the face in the z-direction. Thus, the point of the calculation was to determine that the temperature of the face would be raised and that the time could be reduced with this method. More investigation would need to be done on this potential design; however, this shows that the temperature of the material could be raised and the cycle time reduced using this heating method.

4. VERIFICATION & VALIDATION

For the verification of the accuracy of this program, the finite equations were verified, the stability of the Fourier Number was checked, the number of nodes was verified to be sufficient along with the time step, and the temperature distribution results were compared to temperature distribution images taken from a thermal camera.

4.1 Finite Difference Equations

While building the model, the MATLAB code was continuously checked and debugged. The finite difference equations were verified by checking for convergence. To do this, the boundary conditions were changed to temperature prescribed boundaries at the corners and edges. All of the boundaries were prescribed with the same value for the temperature. The program time was then increased to an infinitely long time. After running, the temperature distribution converged to the boundary temperature throughout the weld face. By converging, this ensured that the finite difference equations were working properly.

4.2 Fourier Number Stability

Based on the finite difference equations, the Fourier Number needed to be less than ¼ for stability. It was desired for the program to calculate the finite difference equations with minimal error. Thus, it was chosen for the Fourier Number to be less than 0.1. In the program, there is a section of the code built in to check the stability of the model based on the Fourier Number. The section of code for the stability check was as shown below:

```
if max(Fo) > 0.1 % Check Stability Criterion for Fourier Number
msg = 'Fourier Number Unstable'; % Error Message
error(msg);
end
```

To verify that this section of code was working, the program was run with a time step, $dt = 1s$. With a 1s time step, the program was stopped and gave an error message indicating that the Fourier number was unstable. This ensures that the program will stop anytime the Fourier number is

greater than 0.1. With the model at its typical time step value of $dt = 0.1s$, the model was stable and did not give the corresponding alarm.

4.3 Mesh Size

In addition to checking the time step, the number of nodes used for the mesh size was checked to ensure the chosen number of nodes did not have a significant effect on the results of the model. The model was calculated with varying mesh sizes and the results compared.

Table **3** below displays the results from the tests varying the mesh size.

Table 3: Effect of the mesh size on the corresponding temperature difference in the adiabatic face of PTFE

N+1	M+1	DIFFERENCE IN L (INCH)	ΔT OF ADIA FACE
36	74	1.39E-03	19.9961
37	76	6.76E-04	20.0410
38	78	0.00E+00	20.0525
39	80	-6.41E-04	20.0924
40	82	-1.25E-03	20.1024

In this table, N+1 and M+1 are the numbers of nodes in the Y and X directions, respectively. N is input into the model and M is calculated based on the value for dx. The total number of nodes for each direction is N+1 and M+1 because of the way the model calculates the nodes. The table also displays the difference in L, or the difference in the length in the X direction based on the difference between the actual length and the calculated length based on the number of nodes. The goal was to minimize this difference in order to have the most accurate calculations. From the table, the error was minimized with the total number of nodes in the Y direction equal to 38, or N=37 input into the model. The number of nodes increased the resolution in the mesh grid for the simulation.

4.4 Time Step

Next, the model was calculated with varying values for the time step to verify that the time step was sufficiently small. The values tested for the time step were bound by the Fourier number stability and a realistic calculation time. To compare results, the temperature difference of the adiabatic face was compared for each calculation. The results are shown in Table 4.

Table 4: Effect of the time step on the temperature difference of the adiabatic face of PTFE

Time Step, dt [s]	Temperature, ΔT of Adiabatic Face [°C]
0.15	Fourier Number Unstable
0.14	NA – creates a total time that is not an integer
0.13	NA – creates a total time that is not an integer
0.12	20.0524
0.11	NA – creates a total time that is not an integer
0.1	20.0525
0.09	20.0525
0.08	20.0526
0.07	NA – creates a total time that is not an integer
0.06	20.0527
0.05	20.0527
0.04	20.0527
0.03	20.0528
0.02	20.0528
0.01	20.0529

As shown, when the time step was equal to 0.15 s, the Fourier Number became unstable. Thus, any time step greater than 0.15 s would have also been unstable. Some of the numbers listed in the table were marked as NA. This is because the model calculates the total number of for loop iterations to run based on the time step. For example, for a total run time of 90 minutes, or 5400 s, the model calculates the total number of time steps using the following equation:

$$time = 5400/dt \tag{16}$$

Time equals the number of time steps that the code iterates through its temperature calculation. Thus, if the time step is equal to 0.14, then $time = \frac{5400}{0.14} = 38{,}571.43$. The number

of times that the model iterates in the temperature distribution calculation must be an integer or MATLAB will give an error. Therefore, any non-integer values were not viable. However, the values that did give integers had very little variance between them with only 0.0005 difference between the maximum and minimum temperature distribution values. With such little variance, it was determined that the time step with any of these values was adequate. A value of dt = 0.1s was used for the results because it is a round number and gave satisfactory accuracy for the calculations. Once the time step and mesh size were verified as accurate and not having a significant effect on the calculations, the temperature distribution was analyzed.

4.5 Process Results vs Predicted Results

To verify that the numerical MATLAB model accurately predicted the temperature distribution in the material, the predicted values were compared to the actual process to calibrate the model. A thermal imaging camera was used to gather temperature distribution results from the actual process. Four tests were completed using the thermal imaging camera. For each test, the material was heated to a specified time of the cycle, then the process was stopped, the material was immediately pulled apart, and thermal images were taken of the cross section of the weld face of the PTFE material. Next are the tests that were done using the thermal camera in Table 5.

Table 5: Test summary of tests done using the thermal camera

Test #	**1**	**2**	**3**	**4**
Material	PTFE	PTFE	PTFE	PTFE
Welder	C	C	D	D
Time	90 min	90 min	90 min	15 min
PFA	Yes	Yes	No	No

Three of the tests involved heating the material through all 90 minutes of the weld cycle, while the fourth test involved heating the material for only 15 minutes of the weld cycle. For these tests, the setup of the process was the same as used for manufacturing pieces with the exception to using PFA between the faces of PTFE. The initial two tests used PFA film between the faces of material; however, the results were deemed inaccurate as they showed the temperature of the PFA rather than the temperature of the PTFE as the program calculates. Therefore, the tests used for

validation of the program did not use PFA film in between the pieces of PTFE. The tests with PFA could still be useful for future process investigation; however, they were not used for the validation of this program. Thus, the validation was based on Test 3 and Test 4 at 90 minutes and 15 minutes, respectively.

The tests were performed using a FLIR 62101-0301 T440 high-sensitivity infrared thermal imaging camera with a temperature range of -4° F to 2192° F. With the maximum needed temperature of 700°F, this was well within the range of what the camera was capable of. In this range, the camera has an error of ±2% or a 2°C accuracy. Images were taken with this camera and then uploaded into the FLIR thermal imaging software where spot measurements could be taken at different points throughout the material. This software was used to place spot measurements at various points along the centerline of the material in order compare the temperatures to the adiabatic face in the MATLAB model. To clarify, the adiabatic face in the MATLAB model is the left face of the simulation area, but not the left face of the PTFE bar. The simulation area is of only half of the bar and thus when the left face is referred to, it refers to the left face of the simulation area. Comparisons were made between the thermal images of the process data and the temperature distribution outputs from the MATLAB model at both the 90-minute and 15-minute intervals. Below are the comparisons between the MATLAB model and the thermal imaging camera results for both time intervals. First is the result from the thermal imaging camera for 15 minutes of the weld cycle in Figure 52.

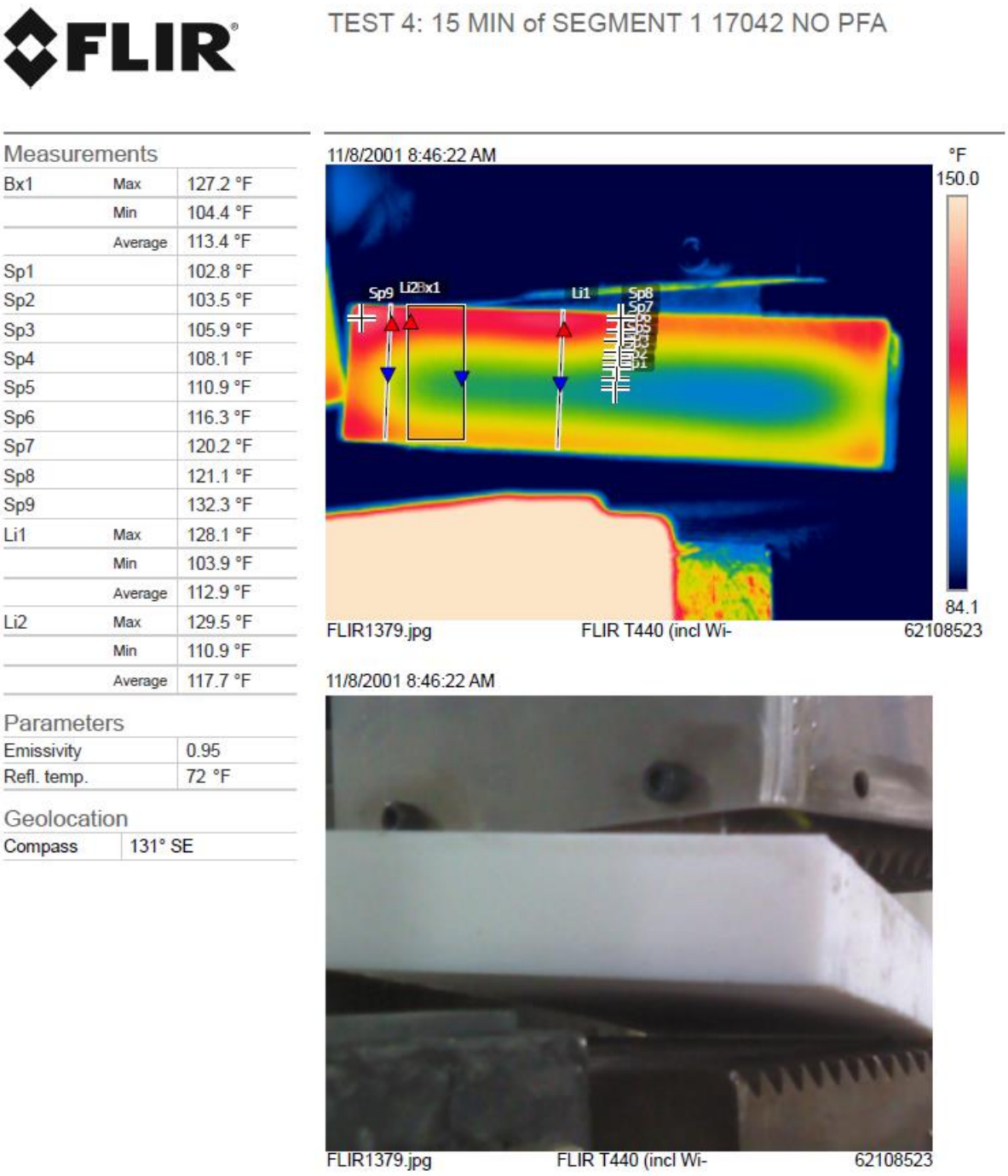

Figure 52: Test 4: FLIR thermal image results: 15 min cycle of segment 1

The results from the FLIR software were in units of Fahrenheit and were converted to Celsius to be compared to the results from the MATLAB model. The results from the MATLAB model are shown in Figure 53.

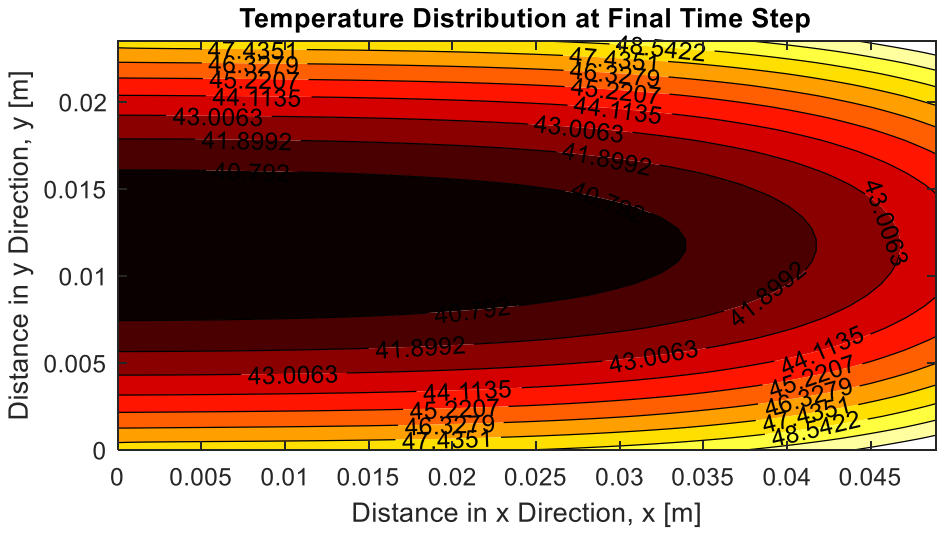

Figure 53: Temperature distribution from MATLAB model after 15 minute interval

The MATLAB prediction results were compared to the data from the thermal camera at two key points: 1) the center of the material and 2) the top of the material, both at the left face of the simulation area, or the adiabatic face in the center. This comparison is shown below in Table 6.

Table 6: 15 min comparison between MATLAB model and thermal camera process data

TEMPERATURE READINGS FROM FLIR CAMERA				
T [°F]	**T [°C]**		**MATLAB**	**% Error**
121.1	49.5	Top Left Node	48.0	**3.1%**
120.2	49.0			
116.3	46.8			
110.9	43.8			
108.1	42.3			
105.9	41.1			
103.5	39.7			
102.8	39.3	Center Left Node	39.7	**-0.9%**
ΔT [°C]	10.17		8.3	**18.4%**

As shown, for the first 15 minutes of the weld cycle, the percent error was 3.1% for the top left node and 0.1% for the center left node. These two main nodes were chosen because they

display the temperature difference throughout the material and show that the maximum temperature is at the boundary. In this case, the thermal camera showed that the temperature difference was larger than what the MATLAB model predicted, and the temperature of the top left node was greater than what was predicted. This could mean that the heat flux in the MATLAB model should be increased. However, there is potential error in the readings from the thermal camera and there is error in the method of taking a picture using the thermal camera. This will further be discussed after the results for Test 3. In test 3, the total 90-minute segment of the weld cycle was setup and run. The result from the thermal camera is shown below in Figure 54.

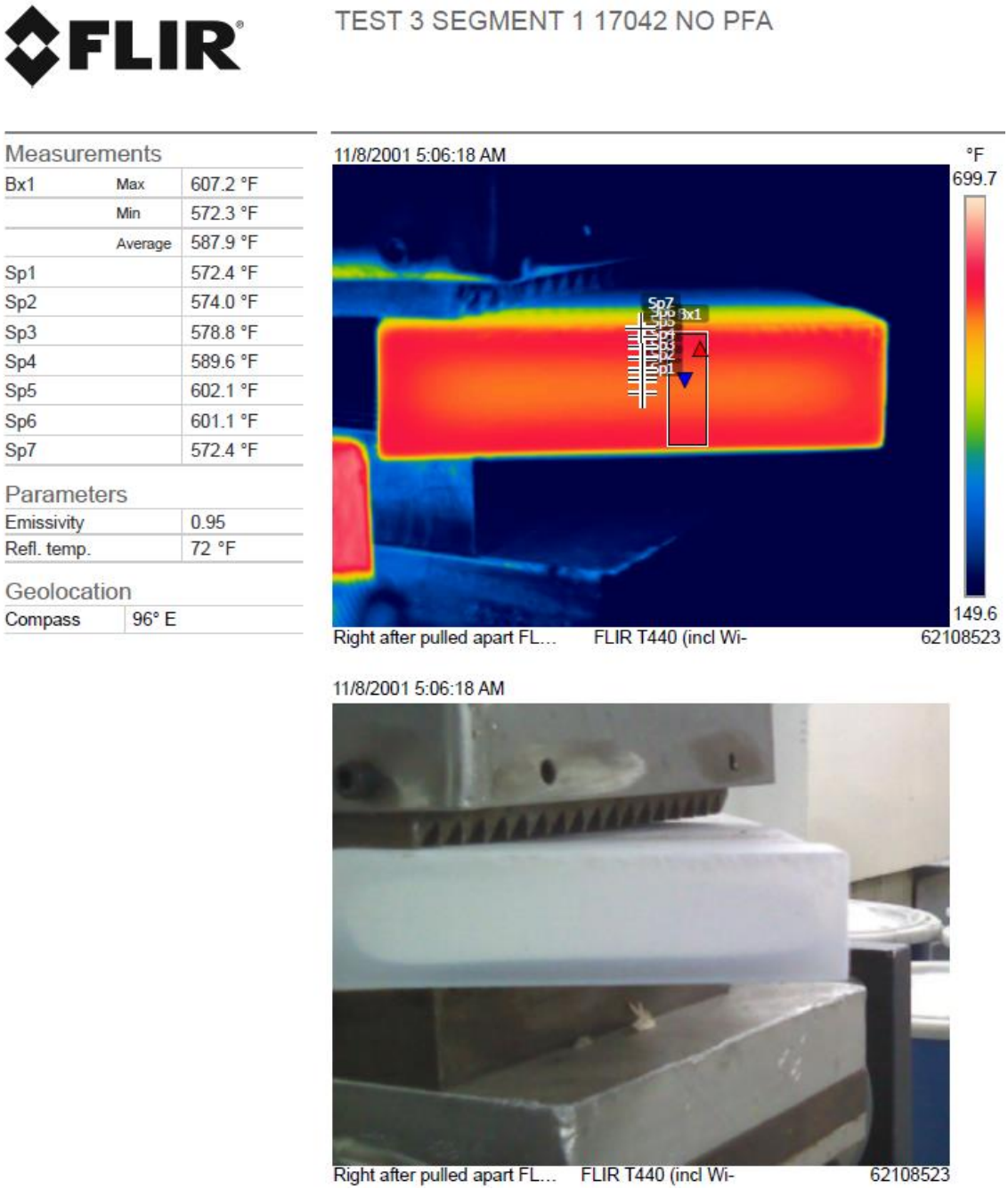

Figure 54: Test 3: FLIR thermal image results: 90 min cycle of segment 1

Similar to Test 4, temperature readings were taken as spot measurements along the centerline of the material or the adiabatic face in the simulation area. These were then compared to the results from MATLAB. The temperature distribution from the MATLAB model is shown in Figure 55.

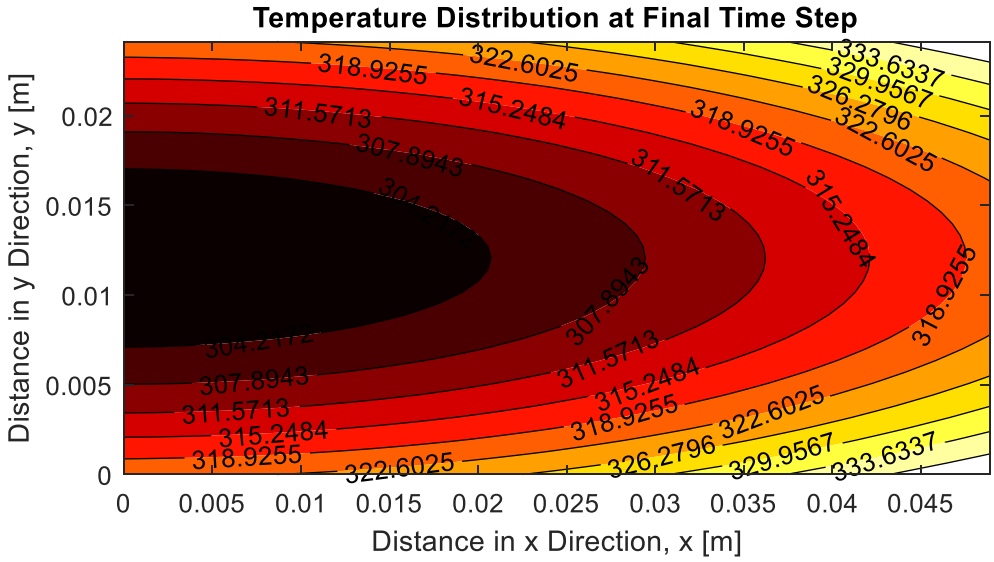

Figure 55: Temperature distribution from MATLAB model for 90 min of segment 1

Both the thermal image and the contour map of the predicted temperature distribution from MATLAB show the same general distribution as the material is colder in the center. The temperatures on the boundaries are much hotter than the center of the material. The temperatures were taken and compared to the MATLAB model as shown below in Table 7.

Table 7: 90 min comparison between thermal camera process data and MATLAB model results

TEMPERATURE READINGS FROM FLIR CAMERA				
T [°F]	**T [°C]**		**MATLAB**	**% Error**
607.2	319.56	Top Left Node	321.4	**-0.6%**
602.1	316.72			
589.6	309.78			
578.8	303.78			
574.0	301.11			
572.4	300.22	Center Left Node	301.3	**-0.36%**
ΔT [°C]	19.33		20.1	**-3.72%**

The temperature difference predicted by the MATLAB model was higher than the difference shown from the thermal image. This was opposite of the data in Test 4. The accuracy of the program however to the thermal camera data was extremely low percent error.

A summary of Test 3 and Test 4 results are shown in Table 8. The comparisons are shown for the top left and center left nodes for the MATLAB prediction versus the result from the thermal camera.

Table 8: Summary comparison between MATLAB model & thermal camera results

		Top Left Node T [°C]	***Center Left Node T [°C]***	***ΔT [°C]***
Test 3	**MATLAB**	321.4	301.3	20.1
	Actual	319.6	300.22	19.33
	% Error	**-0.60%**	**-0.36%**	**-3.72%**
Test 4	**MATLAB**	48.0	39.7	8.67
	Actual	49.5	39.3	10.17
	% Error	**3.10%**	**-0.90%**	**18.4%**

The validation for the accuracy of the MATLAB model was based on these two tests. The time intervals were at times of 15 minutes and 90 minutes of segment 1. Based on the percent error, the program appeared to be an accurate representation of the actual process. For further validation, the program should be compared to thermal imaging results at more time points. Additional validation could be attained using thermocouples at different points in the PTFE bar. It is also important to note that when the thermal images were taken, the PTFE was losing heat. The images were taken very soon after pulling the PTFE pieces apart, so it was assumed that not enough heat was lost to affect the temperature readings. More investigation should be done on the best way to acquire the temperature of the material throughout the process.

5. SUMMARY & CONCLUSION

In summary, this project analyzed the welding process for large diameter PTFE parts for a manufacturer of PTFE seals. The overall goal was to determine if the welding cycle time could be reduced and still ensure a quality weld. To determine the feasibility, the current process was analyzed using a simulation model in MATLAB. This program was able to predict the transient temperature distribution at the weld face of the PTFE using the finite difference method. The material used for the simulation was virgin PTFE.

- Material properties – the specific heat, thermal conductivity, and density were important for this process because the temperature of the PTFE is raised above its melting point during the weld process. For this reason, it was decided to create a unique model capable of calculating the transient material properties. There are programs available for 2-D transient heat transfer; however, these are typically for applications with constant material properties. Thus, a unique model for the process was created in MATLAB with transient material properties using the finite difference method. The density of PTFE varies significantly with temperature and thus justifies the building of a unique model of the process. The model was used to simulate results for a) the current process b) the current process with increased power, and c) the current process with the addition of a center heater.
- Current process – The MATLAB model of the PTFE welding process predicted the temperature distribution at time intervals of 15-minutes and 90-minutes to within 3.1% error of the temperatures of the compared nodes. The nodes compared were the top and center nodes along the adiabatic face of the material. These nodes were chosen because it was desired to know the temperature at the boundary, the temperature in the center of the material, and the temperature difference between the two. The model of the current process showed that the center of the material is cooler than the surrounding boundaries. It also showed that the current heating process heats the weld face unevenly and takes too long.
- Increased power – Results were also simulated for the welding process with increased heater power. With increased power, the temperature throughout the material was raised; however, the temperature difference from the top node to the center node was also increased. With an increased temperature difference, the temperature in the center of the

material would likely not be hot enough for a sufficient weld. More investigation would need to be done on the weld cycle times if the heater power was increased. However, from preliminary results, the boundaries would be heated too quickly, and the center would not be hot enough. Simply adding more power would not be an ideal solution because the temperature difference in the material would increase.

- Hot plate welding method – a semi-infinite heat flux analysis was performed to simulate the results for the addition of a heater between the two faces of material much like a hot plate welding method. The results showed that the temperature of the face of the material could be raised approximately 57°C by using 100W for the 90-minute segment of the weld cycle. This means that the 90-minute cycle could be reduced to about 77.5 minutes and still reach the same temperature. Though this is not a major time reduction, this type of heating process would ensure that the material would be heated evenly along the entire weld face. This welding method would have to be investigated further for the use of PFA between the two pieces of PTFE, but the results show that this method would heat the material evenly compared to the current process.

6. FURTHER STUDY & RECOMMENDATIONS

The goal of this study was to develop an accurate model of the current process for future design improvements. Though this objective was completed, there are many other areas which need to be further understood and investigated.

- Model optimization – the MATLAB model accurately predicts the solution for the current process; however, it could be optimized to be used as a design change tool. The computation time of the current model should be reduced to under 5 seconds by reducing the amount of data that is stored.
- Model Capabilities – The current model calculates the solution for one segment of the main program. The appropriate code should be added so that it is capable of including additional segments of the program. It would also be useful to have a model that is capable of using any welding cycle, using the program number as an input to calculate the corresponding solution. In addition, the model should have the material as an input and use the corresponding material properties based on the specified material.
- PFA welding properties - To be a completely accurate tool for optimization, it would be desirable to have the model calculate the temperature of the PFA material as well. As mentioned in Section 2.2.5 about the current welding method, two pieces of PFA film are inserted in between the pieces of PTFE to be welded. For the MATLAB model and the Validation using the thermal camera, the PFA was disregarded because the goal was to examine the behavior of the PTFE. However, because PFA is used in the actual process, it would be useful to model the melting of the PFA film as well as the temperature of the PTFE weld face.
- Process Validation – The heating process should be further investigated to be fully understood. The model should be further verified with temperature data throughout the process. More images should be taken with the thermal camera at various time points, and data should be collected from thermocouples on both the PTFE and the heaters. More examination should be done to determine how much heat is lost and what the actual heat flux on the material is. This could help determine if design changes to insulate the welders would have a dramatic effect.

- Material properties – The material properties of PTFE are extremely complex and should be further investigated for the applicability during this welding process. In conjunction to the material properties, more examination on the melting point and phase change of PTFE should be conducted. This model attempted to incorporate the melting by using temperature dependent material properties, but the melting of PTFE is a complex phenomenon. When it begins to melt, PTFE greatly expands volumetrically. This could change the heat that is input into the material by changing the surface area in contact with the heater dies. This model incorporated a basic temperature dependence; however, much more could be done to examine the thermal expansion and melting of PTFE.
- Design changes – Finally, further study should be done on the potential design improvements that could be implemented. This project showed that the cycle time could be reduced by placing a heater in between the faces of the PTFE. This potential design would be similar to a hot plate welding method and should be evaluated further to determine if it is a feasible solution. It should also be analyzed to see if the PFA would work with this design or if it would stick to the center heater as that is one of the biggest concerns of this potential design. This type of heating is recommended as it will heat the PTFE weld face more evenly and ensure that the entire face is at the desired temperature. It is recommended that once a new design is implemented, an optimization study should be performed to ensure that the settings give the best possible weld.

This study provided an immense amount of insight into understanding the current process. Though there are many areas that are recommended to be investigated further, the model presented in this thesis is thought to be an accurate representation of the current welding process. The results from this study will be a vital tool to be used for further design investigation. Having a design tool will save the company time and money that would otherwise be spent on a trial and error process determining the best solution. This project also provides the company a comprehensive documentation on the current welding process. The results presented in this thesis will further be utilized to suggest design changes, implementation, and optimization of the PTFE welding machines.

APPENDIX

Table 9: Determination of the mesh grid size with the highest resolution

N+1	dy [m]	dx [m]	M+1	Error in L (m)	Error in L (m)
30	8.04E-04	8.04E-04	62	1.69E-04	6.67E-03
31	7.78E-04	7.78E-04	64	1.43E-04	5.65E-03
32	7.54E-04	7.54E-04	66	1.19E-04	4.69E-03
33	7.31E-04	7.31E-04	68	9.62E-05	3.79E-03
34	7.10E-04	7.10E-04	70	7.47E-05	2.94E-03
35	6.89E-04	6.89E-04	72	5.44E-05	2.14E-03
36	6.70E-04	6.70E-04	74	3.53E-05	1.39E-03
37	6.52E-04	6.52E-04	76	1.72E-05	6.76E-04
38	6.35E-04	6.35E-04	78	0.00E+00	0.00E+00
39	6.19E-04	6.19E-04	80	-1.63E-05	-6.41E-04
40	6.03E-04	6.03E-04	82	-3.18E-05	-1.25E-03
41	5.89E-04	5.89E-04	84	-4.65E-05	-1.83E-03
42	5.75E-04	5.75E-04	86	-6.05E-05	-2.38E-03
43	5.61E-04	5.61E-04	88	-7.38E-05	-2.91E-03
44	5.48E-04	5.48E-04	90	-8.66E-05	-3.41E-03
45	5.36E-04	5.36E-04	92	-9.88E-05	-3.89E-03
46	5.25E-04	5.25E-04	94	-1.10E-04	-4.35E-03
47	5.13E-04	5.13E-04	96	-1.22E-04	-4.79E-03
48	5.03E-04	5.03E-04	98	-1.32E-04	-5.21E-03
49	4.92E-04	4.92E-04	100	-1.43E-04	-5.61E-03
50	4.83E-04	4.83E-04	102	-1.52E-04	-6.00E-03

TABLE II
Recommended Thermodynamic Data of Crystalline Polytetrafluoroethylene

T (K)	C_p (J mol^{-1} K^{-1})	$H^c_T - H^c_0$ (J mol^{-1})	S^c_T (J mol^{-1} K^{-1})	$-(G^c_T - H^c_0)$ (J mol^{-1})
0.0	0.0	0.0	0.0	0.0
0.3	0.0000649	0.00000974	0.00003246	0.0
0.4	0.0001249	0.00001923	0.00005889	0.0000043
0.5	0.0002226	0.00003660	0.00009676	0.0000118
0.6	0.0003704	0.00006625	0.0001499	0.0000237
0.7	0.0005816	0.0001139	0.0002223	0.0000418
0.8	0.0008707	0.0001865	0.0003183	0.0000681
0.9	0.001252	0.0002926	0.0004422	0.0001054
1.0	0.001740	0.0004422	0.0005988	0.0001566
1.2	0.003094	0.0009256	0.0010306	0.0003111
1.4	0.005041	0.001739	0.001649	0.0005688
1.6	0.007687	0.003012	0.002489	0.0009706
1.8	0.01111	0.004892	0.003587	0.001564
2.0	0.01538	0.007541	0.004973	0.002405
3.0	0.05071	0.04059	0.01727	0.01122
4.0	0.1086	0.1202	0.03930	0.03694
5.0	0.2284	0.2887	0.0757	0.08982
10.0	1.228	3.930	0.4969	1.039
15.0	2.565	13.41	1.231	5.059
20.0	3.915	29.61	2.148	13.35
25.0	5.155	52.29	3.153	26.54
30.0	6.301	80.93	4.194	44.89
40.0	8.441	154.6	6.299	97.32
50.0	10.31	248.4	8.385	170.9
60.0	12.27	361.3	10.44	265.0
70.0	14.17	493.5	12.47	379.6

80.0	16.02	644.4	14.49	514.5
90.0	17.75	813.3	16.47	669.4
100.0	19.37	998.9	18.43	844.0
110.0	21.20	1202	20.36	1038
120.0	22.90	1422	22.28	1251
130.0	24.53	1659	24.18	1484
140.0	26.13	1913	26.05	1735
150.0	27.65	2182	27.91	2005
160.0	29.13	2465	29.74	2293
170.0	30.62	2764	31.55	2599
180.0	31.98	3077	33.34	2924
190.0	33.24	3403	35.10	3266
200.0	34.47	3742	36.84	3626
210.0	35.67	4093	38.55	4003
220.0	36.82	4455	40.24	4397
230.0	37.94	4829	41.90	4808
240.0	39.03	5214	43.54	5235
250.0	40.10	5609	45.15	5678
260.0	41.13	6015	46.74	6138
270.0	42.15	6432	48.32	6613
273.15	42.47	6565	48.81	6766
280.0	43.15	6858	49.87	7104
290.0	44.13	7295	51.40	7611
292.0 (T_c)	44.32	7383	51.70	7714
292.0	44.32	8097	54.15	7714
298.15	44.91	8372	55.08	8050
300.0	45.09	8455	55.36	8152
303.0 (T_c)	45.37	8591	55.81	8318

TABLE II (continued)

303.0	45.37	8727	56.25	8318
310.0	46.02	9047	57.30	8716
320.0	46.95	9511	58.77	9296
330.0	47.86	9985	60.23	9891
340.0	48.76	10,469	61.68	10,501
350.0	49.63	10,960	63.10	11,125
360.0	50.49	11,461	64.51	11,763
370.0	51.35	11,970	65.91	12,415
380.0	52.17	12,488	67.29	13,081
390.0	52.99	13,014	68.65	13,761
400.0	53.81	13,548	70.00	14,454
410.0	54.60	14,090	71.34	15,161
420.0	55.39	14,640	72.67	15,881
430.0	56.15	15,197	73.98	16,614
440.0	56.91	15,763	75.28	17,361
450.0	57.65	16,335	76.57	18,120
460.0	58.39	16,916	77.84	18,892
470.0	59.10	17,503	79.11	19,677
480.0	59.82	18,098	80.36	20,474
490.0	60.51	18,699	81.60	21,284
500.0	61.20	19,308	82.83	22,106
510.0	61.88	19,923	84.05	22,940
520.0	62.55	20,545	85.25	23,787
530.0	63.20	21,174	86.45	24,646
540.0	63.86	21,810	87.64	25,516
550.0	64.48	22,451	88.82	26,398
560.0	65.12	23,099	89.99	27,292
570.0	65.75	23,754	91.14	28,198
580.0	66.36	24,414	92.29	29,115
590.0	66.96	25,081	93.43	30,044
600.0	67.58	25,753	94.56	30,984
605.0 (T_m)	67.88	26,092	95.12	31,458
610.0	68.18	26,432	95.68	31,935
620.0	68.77	27,117	96.80	32,898
630.0	69.35	27,808	97.90	33,871
640.0	69.93	28,504	99.00	34,856
650.0	70.50	29,206	100.1	35,851
660.0	71.06	29,914	101.2	36,857
670.0	71.64	30,627	102.2	37,875
680.0	72.19	31,347	103.3	38,902
690.0	72.75	32,073	104.4	39,941
700.0	73.30	32,802	105.4	40,990

Figure 56: Recommended data for specific heat capacity of PTFE: (Lau et al., 1984)

Table 10: Calculation of mass based specific heat from given molar specific heat

T [K]	T [°C]	Cp [J/mol-K]	Cp [J/kg-K]
290	16.85	44.13	441.23
292	18.85	44.32	443.13
298.15	25	44.91	449.03
300	26.85	45.09	450.83
303	29.85	45.37	453.63
310	36.85	45.09	450.83
320	46.85	46.02	460.13
330	56.85	46.02	460.13
340	66.85	46.95	469.43
350	76.85	47.86	478.53
360	86.85	48.76	487.53
370	96.85	49.63	496.23
380	106.85	50.49	504.82
390	116.85	52.99	529.82
400	126.85	53.81	538.02
410	136.85	54.6	545.92
420	146.85	55.39	553.82
430	156.85	56.15	561.42
440	166.85	56.91	569.01
450	176.85	57.65	576.41
460	186.85	58.39	583.81
470	196.85	59.1	590.91
480	206.85	59.82	598.11
490	216.85	60.51	605.01
500	226.85	61.2	611.91
510	236.85	61.88	618.71
520	246.85	62.55	625.41
530	256.85	63.2	631.91
540	266.85	63.86	638.50
550	276.85	64.48	644.70
560	286.85	65.12	651.10
570	296.85	65.75	657.40
580	306.85	66.36	663.50
590	316.85	66.96	669.50
600	326.85	67.58	675.70
605	331.85	67.88	678.70
610	336.85	68.18	681.70
620	346.85	68.77	687.60
630	356.85	69.35	693.40

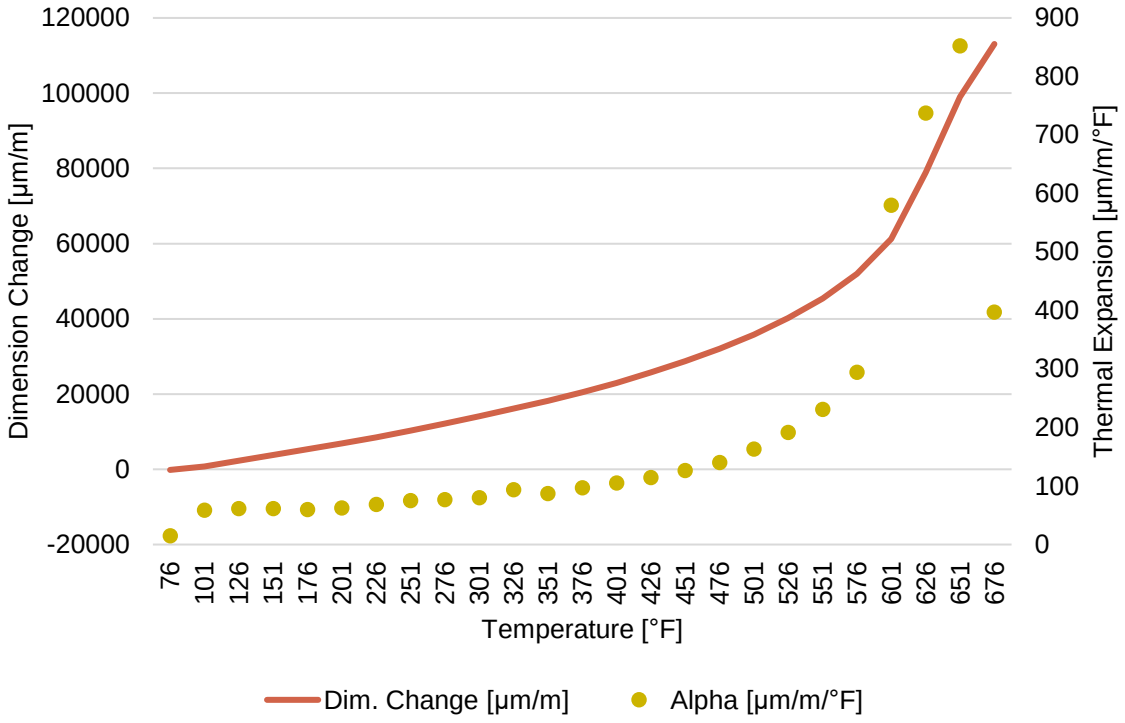

Figure 57: Transient dimensional change data and thermal expansion used to calculate the transient density response for virgin PTFE

Table 11: Calculation of density for virgin PTFE from thermal expansion data

T [°F]	T [°C]	T [K]	Dim. Change [µm/m]	Alpha [µm/m/°F]	Alpha [m/m/°F]	Volume [m^3]	Density [kg/m^3]
76	24.44	297.59	-167.8	14.81	1.48E-05	1.29E-04	2159.55
101	38.33	311.48	772.2	58.31	5.83E-05	1.30E-04	2149.42
126	52.22	325.37	2311	61.08	6.11E-05	1.31E-04	2139.18
151	66.11	339.26	3848	61.44	6.14E-05	1.31E-04	2129.34
176	80.00	353.15	5351	59.33	5.93E-05	1.32E-04	2121.06
201	93.89	367.04	6866	62.1	6.21E-05	1.33E-04	2109.65
226	107.78	380.93	8491	68.28	6.83E-05	1.34E-04	2094.33
251	121.67	394.82	10283	75.04	7.50E-05	1.35E-04	2076.77
276	135.56	408.71	12189	76.36	7.64E-05	1.35E-04	2064.00
301	149.44	422.59	14120	79.63	7.96E-05	1.36E-04	2048.42
326	163.33	436.48	16136	93.34	9.33E-05	1.39E-04	2017.12
351	177.22	450.37	18152	87.11	8.71E-05	1.39E-04	2013.71
376	191.11	464.26	20456	96.92	9.69E-05	1.41E-04	1985.14
401	205.00	478.15	22983	105.2	1.05E-04	1.43E-04	1957.42
426	218.89	492.04	25731	114.3	1.14E-04	1.45E-04	1926.83
451	232.78	505.93	28730	126.1	1.26E-04	1.48E-04	1889.84
476	246.67	519.82	32024	140.1	1.40E-04	1.51E-04	1847.22
501	260.56	533.71	35798	162.8	1.63E-04	1.56E-04	1786.67
526	274.44	547.59	40219	191.6	1.92E-04	1.63E-04	1713.91
551	288.33	561.48	45452	230.8	2.31E-04	1.72E-04	1623.07
576	302.22	575.37	51936	294.3	2.94E-04	1.87E-04	1495.97
601	316.11	589.26	61242	579.4	5.79E-04	2.48E-04	1126.61
626	330.00	603.15	78891	737.4	7.37E-04	2.88E-04	971.80
651	343.89	617.04	98989	851.8	8.52E-04	3.21E-04	872.29
676	357.78	630.93	113067	396.9	3.97E-04	2.22E-04	1257.51

Table I Some key properties of PTFE given

Properties	DIN or ASTM Standard	Unit	PTFE Typical Value
PHYSICAL			
Specific gravity	ASTM D 792	g/cm^3	2.17
Max. working temperature	-	°C	260
Water absorption	53495	%	<0.03
MECHANICAL			
Tensile strength @ 23° C	ASTM D 4894	MPa	29-39
Yield point	ASTM D 4894	N/mm^2	10
Elongation at break	ASTM D 4894	%	200-500
Ball hardness	ISO 2039-1	N/mm^2	25-30
Shore hardness D	ASTM D 2240	N/mm^2	55-72
Coefficient off riction (dry steel)	-	-	0.05-0.2
THERMAL			
Melting temperature	ASTM 2116	°C	327
Coefficient of expansion	ISO 11359-2	1/K	1E-4
Thermal conductivity @ 23° C	52612	W/m/K	0.23
Specific heat @ 23° C	-	J/g/K	0.01
ELECTRICAL			
Dielectric constant	53483	-	2.0-2.1
Surface resistivity	DIN 53482	Ohm	5E+17
Arch resistance	ASTM 495	Sec.	>360
Dielectric strength	53481	KV/mm	40-80

Note: The exact values may vary with grade and producer.
The data is taken from manufacturing data, gathered by Adtech and TSSH.

Figure 58: Data for virgin PTFE at 23°C

Physical Properties	Metric	English	Comments
Density	8.41 g/cc	0.304 lb/in³	
Mechanical Properties	**Metric**	**English**	**Comments**
Hardness, Rockwell B	78	78	
Tensile Strength, Ultimate	476 MPa	69000 psi	
Tensile Strength, Yield	317 MPa @Strain 0.500 %	46000 psi @Strain 0.500 %	
Elongation at Break	27 %	27 %	In 50 mm
Reduction of Area	50 %	50 %	
Modulus of Elasticity	100 GPa	14500 ksi	
Poissons Ratio	0.28	0.28	calculated
Fatigue Strength	100 MPa @# of Cycles 3.00e+8	14500 psi @# of Cycles 3.00e+8	source does not state temper
Machinability	30 %	30 %	UNS C36000 (free-cutting brass) = 100%
Forgeability	90 %	90 %	UNS C37700 (forging brass) = 100%
Shear Modulus	39.0 GPa	5660 ksi	
Shear Strength	296 MPa	42900 psi	
Electrical Properties	**Metric**	**English**	**Comments**
Electrical Resistivity	0.00000663 ohm-cm @Temperature 20.0 °C	0.00000663 ohm-cm @Temperature 68.0 °F	
Thermal Properties	**Metric**	**English**	**Comments**
CTE, linear	21.2 µm/m-°C @Temperature 20.0 - 300 °C	11.8 µin/in-°F @Temperature 68.0 - 572 °F	
Specific Heat Capacity	0.380 J/g-°C	0.0908 BTU/lb-°F	
Thermal Conductivity	116 W/m-K @Temperature 20.0 °C	805 BTU-in/hr-ft²-°F @Temperature 68.0 °F	
Melting Point	885 - 900 °C	1630 - 1650 °F	
Solidus	885 °C	1630 °F	
Liquidus	900 °C	1650 °F	
Processing Properties	**Metric**	**English**	**Comments**
Annealing Temperature	425 - 600 °C	797 - 1110 °F	
Hot-Working Temperature	650 - 825 °C	1200 - 1520 °F	
Recrystallization Temperature	350 °C	662 °F	For 19 mm diameter rod cold drawn 30%

Figure 59: Naval brass properties for heater dies (Davis et al. 2001)

www.matweb.com/search/datasheet_print.aspx?matguid=c3bea3ce78e34dea82cd2fd16b0e5abf

ASM Specialty Handbook - Copper and Copper Alloys, edited by Joseph R. Davis, Davis & Associates, ASM International, Metals Park, OH, (2001).

REFERENCES

Ajroldi, G., Garbuglio, C., & Ragazzini, M. (1970). Some Rheological Properties of Molten Polytetrafluoroethylene. *Journal of Applied Polymer Science, 14*, 79-88.

Anca, A., Cardona, A., Risso, J., & Fachinotti, V. D. (2011). Finite Element Modeling of Welding Processes. *Applied Mathematical Modelling, 35*, 688-707.

Araki, Y. (1965). Thermal Expansion Coefficient of Polytetrafluoroethylene in the Vicinity of Its Glass Transition at about 400 K. *Journal of Applied Polymer Science, 9*, 421-427.

B.G. THOMAS, I. S. (1984). Comparison of Numerical Modeling Techniques for Complex, Two-Dimensional, Transient Heat-Conduction Problems. *Metallurgical Transactions B, 15B*, 307-318.

BASF. (2003). *JOINING OF NYLON BASED PLASTIC COMPONENTS -- VIBRATION AND HOT PLATE WELDING TECHNOLOGIES.* Mount Olive, NJ: BASF Corporation.

BASF;. (2003). *Innovations in Laser Welding of Thermoplastics: This Advanced Technology is Ready to be Commercialized.* Mount Olive, NJ: Society of Automotive Engineers, Inc.

Benatar, A. (2015). Ultrasonic Welding of Plastics and Polymeric Composites. *Power Ultrasonics: Applications of High Intensity Ultrasound*, 295-312.

Benatar, A. (2017). Plastics Joining. In M. Kutz, *Applied Plastics Engineering Handbook, Processing, Materials, and Applications* (pp. 575-591). Waltham: William Andrew.

Biron, M. (2018). *Thermoplastics and Thermoplastic Composites.* William Andrew.

Blumm, J., Lindemann, A., Meyer, M., & Strasser, C. (2010). Characterization of PTFE Using Advanced Thermal Analysis Techniques. *Int J Thermophys, 31*, 1919-1927.

Boyard, N. (2016). Heat Transfer in Polymer Composite Materials. *Forming Processes*, 1-31.

Bucknall, C. B., Drinkwater, I. C., & Smith, G. R. (1980, April). Hot Plate Welding of Plastics: Factors Affecting Weld Strength. *Polymer Engineering and Science, Vol. 20*(No. 6), 432-440.

Castleman, L. (2015). Simulating Seal Life with Finite Element Analysis. *BioProcess International*.

Council, A. C. (2018). *The Basics: Polymer Definition and Properties*. Retrieved from https://plastics.americanchemistry.com/plastics/The-Basics/

Cui, M., Xu, B.-B., Lv, J., Gao, X.-W., & Zhang, Y. (2018). Numerical solution of multi-dimensional transient nonlinear heat conduction problems with heat sources by an extended element differential method. *International Journal of Heat and Mass Transfer, 126*, 1111-1119.

Dodiuk, H., & Goodman, S. H. (2014). *Handbook of Thermoset Plastics.* William Andrew.

Drobizhev, A., Reiten, J., Singh, V., & Kolomensky, Y. G. (2017). Thermal conductivity measurements of PTFE and Al2O3 ceramic at sub-Kelvin temperatures. *Cryogenics, 85*, 63-70.

Dupont. (n.d.). *Teflon PTFE Fluoropolymer Resin Properties Handbook.* Wilmington, DE.

Ebnesajjad, S. (2015). *Fluoroplastics Volume 1: Non-Melt Processible Fluoropolymers - The Definitive User's Guide and Data Book.* Waltham, MA: William Andrew.

Ebnesajjad, S. (2015). *FLUOROPLASTICS Volume 2: Melt Processible Fluoropolymers - The Definitive User's Guide and Data Book* (2nd ed., Vol. 2). Waltham, MA: Matthew Deans.

Ebnesajjad, S. (2016). *Expanded PTFE Applications Handbook.* William Andrew.

Farrokhpanah, A., Bussmann, M., & Mostaghimi, J. (2017). New smoothed particle hydrodynamics (SPH) formulation for modeling heat conduction with solidification and melting. *Numerical Heat Transfer, Part B: Fundamentals, 71*, 299-312.

Ferry, L., Vigier, G., Vassoille, R., & Bessede, J. L. (1995). Study of Polytetrafluoroethylene Crystallization. *Acta Polymer, 46*, 300-306.

Furukawa, G. T., McCoskey, R. E., & King, G. J. (1952). Calorimetric Properties of Polytetrafluoroethylene (Teflon) from 0° to 365° K. *Journal of Research of the National Bureau of Standards, 49*(No. 4), 273-278.

Gangal, S. V., & Brothers, P. D. (2010). Perfluorinated Polymers, Polytetrafluoroethylene. *Encyclopedia of Polymer Science and Technology*, 1-26.

Goto, T., & Suzuki, M. (1996). Analysis of transient heat conduction with phase changes by a boundary integral equation method. *Nuclear Engineering and Design, 162*, 317-324.

Grewell, D., & Benatar, A. (2007). Welding of Plastics: Fundamentals and New Developments. *International Polymer Processing XXII*, 43-60.

Grimm, R. A. (2000). Through-Transmission Infrared Welding (TTIR) of Teflon TFE (PTFE). *Society of Plastics Engineers Technical Conference: Plastics, the Magical Solution* (pp. 1143-1147). Orlando, FL: Edison Welding Institute.

Grimm, R. A. (2001). Infrared Welding of Polymers. *Plastics Welding MDDI Online*, 1-7.

Gülkaç, V. (2015, February). An Implicit Finite-Difference Method for Solving the Heat-Transfer Equation. *International Journal of Scientific and Innovative Mathematical Research (IJSIMR), 3*(2), 39-44.

H. W. STARKWEATHER, J. (1982). The Density of Amorphous Polytetrafluoroethylene. *Journal of Polymer Science: Polymer Physics Edition, 20*, 2159-2161.

Hu, T.-Y., & Eiss Jr., N. S. (1983). The Effects of Molecular Weight and Cooling Rate on Fine Structure, Stress-Strain Behavior and Wear of Polytetrafluoroethylene. *Wear, 84*(2), 203-215.

Huang, Y., Meng, X., Xie, Y., Wan, L., Lv, Z., Cao, J., & Feng, J. (2018). Friction stir welding/processing of polymers and polymer matrix composites. *Composites: Part A, 105*, 235-257.

Joseph R. Davis, D. &. (2001). *ASM Specialty Handbook - Copper and Copper Alloys.* Metals Park, OH: ASM International.

Kirby, R. K. (1956, August). Thermal Expansion of Polytetrafluoroethylene (Teflon) From -190° to +300° C. *Journal of Research of the National Bureau of Standards, 57*(No. 2), 91-94.

Kocatüfeka, U., Yenib, Ç., Ülkerc, A., Sayerd, S., & Özdemire, U. (2014). Optimization of hot plate welding parameters of glass fibered reinforced Polyamide 6 (PA6 GF15) composite material by Taguchi method. *Usak University Journal of Material Sciences*, 69-85.

Lau, S. F., Suzuki, H., & Wunderlich, B. (1984). The Thermodynamic Properties of Polytetrafluoroethylene. *Journal of Polymer Science: Polymer Physics Edition, 22*, 379-405.

Lee, I.-G., Kim, D.-H., Jung, K.-H., Kim, H.-J., & Kim, H.-S. (2017). Effect of the cooling rate on the mechanical properties of glass fiber reinforced thermoplastic composites. *Composite Structures, 177*, 28-37.

Liu, K., & Piggott, M. R. (1995). Shear Strenght of Polymers and Fibre Composites: 1. Thermoplastic and Thermoset Polymers. *Composites, Vol. 26*(12), 829-840.

Mehdizadeh, M. (2010). *Microwave/RF Applicators and Probes: for Material Heating, Sensing and Plasma Generation.* San Diego: William Andrew.

Mills, A. F. (1992). *Heat Transfer.* Concord, MA: Richard D. Irwin, Inc.

Nasiri, M. B., & Enzinger, N. (2019, Jan.). Powerful analytical solution to heat flow problem in welding. *International Jounal of Thermal Sciences, 135*, 601-612.

Powell, A. (2002). *Finite Difference Solution of the Heat Equation.*

Price, D. M., & Jarratt, M. (2002). Thermal Conductivity of PTFE and PTFE Composites. *Thermochimica Acta*, 231-236.

Pucciariello, R., & Mancusi, C. (1998). Extreme Thermal Behaviors of Polytetrafluoroethylene and Random Tetrafluoroethylene Fluorinated Copolymers.

Pucciariello, R., & Villani, V. (2004). Melting and Crystallization Behavior of Poly(tetrafluoroethylene) by Temperature Modulated Calorimetry. *Polymer, 45*, 2031-2039.

Pucciariello, R., Villani, V., & Mancusi, C. (1999). On Melt-Crystallization of Polytetrafluoroethylene and of Random Fluorinated Copolymers of Tetrafluoroethylene. *Journal of Applied Polymer Science, 74*, 1607-1613.

Pyda, M. (2013). Melting. In E. Piorkowska, & G. C. Rutledge, *Handbook of Polymer Crystallization* (pp. 265-286). Hoboken, New Jersey: John Wiley & Sons, Inc.

Ritter, G. W., Benatar, A., Grewell, D. A., Messics, J. W., Savitski, A., & Short, M. A. (2015). Plastics. In H. R. Castner, *Welding Handbook Volume 5: Materials and Applications, Pt. 2* (pp. 517-567). American Welding Society.

Sanders, H.-W. (2013). *Slashing Downtime With Innovative Seal Welding Technology*. Trelleborg.

Sojiphan, K., & Benatar, A. (2009). PREDICTION OF RESIDUAL STRESS FORMATION IN POLYCARBONATE WELDED SAMPLES USING ANSYS FINITE ELEMENT SOFTWARE. 1-5.

Soundarrajan, M., Srinivasan, V. R., Maniyarasan, M., & Venkatesh, K. (2014). Design and Modeling of Advanced Welding System for Thermoplastics. *International Journal for Scientific Research & Development, Vol. 2*(09), 286-291.

Starkweather, H. W. (1985). The Effect of Heating Rate on the Melting of Polytetrafluoroethylene. *Journal of Polymer Science: Polymer Physics Edition, 23*, 1177-1185.

Teflon. (2016). *Plastic of the 21st Century*. Retrieved from https://teflon2016.wordpress.com/2016/09/04/chemicool-polytetraflouroethene/

Troughton, M. J. (2008). *Handbook of Plastics Joining.* Norwich, NY: William Andrew.

Vollmond, H. (2017). *PEEK Welding in Zurcon Z431*. Trelleborg.

Woosman, N. M., & Sallavanti, R. A. (2003). *Achievable Weld Strengths for Various Thermoplastics Using the Clearweld Process.* Carbondale, PA: ANTEC.

Zhang, Y., Zhang, D., Wu, J., Li, J., & He, Z. (2017). Non-Fourier Heat Conduction and Phase Transition in Laser Ablation of Polytetrafluoroethylene (PTFE). *Acta Astronautica, 140*, 338-350.

Zhu, X. K., & Chao, Y. J. (2002). Effects of temperature-dependent material properties on welding simulation. *Computers and Structures, 80*, 967-976.

Zunlong, J., Xiaotang, C., Yongqing, W., & Dingbiao, W. (2015). Thermal Conductivity of PTFE Composites Filled with Graphite Particles and Carbon Fibers. *Computational Materials Science, 102*, 45-50.